The Canadian Mineralogist
Vol. 50, pp. 000 (2012)
DOI: 10.3749/canmin.50.4.000

MINERALOGY AND ORIGIN OF THE DUMORTIERITE-BEARING PEGMATITES OF VIRORCO, SAN LUIS, ARGENTINA

MIGUEL ANGEL GALLISKI§ AND MARIA FLORENCIA MÁRQUEZ-ZAVALÍA

IANIGLA, CCT–MENDOZA CONICET, Avda. Ruiz Leal s/n, Parque Gral. San Martín, C.C. 330, (5.500) Mendoza, Argentina

RAÚL LIRA

CICTERRA – CONICET, Museo de Mineralogía y Geología "Dr. A. Stelzner", F.C.E.F y N. Universidad Nacional de Córdoba, Av. V. Sarsfield 299, (5000) Córdoba, Argentina

JAN CEMPÍREK

Department of Mineralogy and Petrography, Moravian Museum, Zelný trh 6, CZ–659 37, Brno, Czech Republic

RADEK ŠKODA

Department of Geological Sciences, Masaryk University, Kotlárská 2, 611 37 Brno, Czech Republic

ABSTRACT

The Virorco dumortierite-bearing pegmatite dikes, in Sierra de San Luis, Eastern Pampean Ranges of central Argentina, are a group of thin, steeply dipping dikes 2 to 10 cm thick with variable lengths (a few dm to <2 m). The pegmatites are emplaced in partially uralitized norite and gabbro that belong to a larger mafic–ultramafic intrusive belt. The pegmatite dikes are symmetrically zoned, with quartz, albite, oligoclase, tourmaline-supergroup and dumortierite-group minerals, muscovite and kyanite as the major phases; the accessory and trace minerals include beryl, chrysoberyl, garnet, fluorapatite, columbite-(Mn) to tantalite-(Mn), pollucite, gahnite, zircon, uraninite and thorite. Holmquistite was found in the exocontact asemblage. Primary textures of magmatic origin were partially disrupted by partial replacements by later minerals and incipient to strong deformation. The whole-rock chemical composition of the dikes shows SiO_2 contents normal for rare-element pegmatites whereas amounts of Al_2O_3 and B_2O_3 are very high. The composition features high MgO, FeO, CaO and P_2O_5 and, for pegmatites, unusually low Na_2O and K_2O contents. Amounts of trace elements are remarkably high in case of Cs (4.3–94.1 ppm), Ta (130–500) and Be (137–261). The normalized REE contents are low (0.1 to 30 times chondrite), highlighted by a strong negative Eu anomaly. Five textural and compositional types of tourmaline-supergroup minerals were identified in the different pegmatitic zones, ranging from dravite-rich compositions to rossmannite, passing through schorl and Mn-rich elbaite. At least four generations of the dumortierite–holtite minerals are texturally and compositionally represented in these dikes: the earliest dumortierite replaces muscovite and tourmaline, locally together with a second generation that grades into As-poor holtite. The third generation is represented by overgrowths or individual crystals of As-poor and As-rich holtite; it is commonly overgrown by the last generation of dumortierite enriched in As. The chemical evolution of dumortierite-group minerals is characterized by an increase of Ta, Nb and minor As, followed by an extensive enrichment in As(+ Sb + Bi) along with gradual decrease in Ta + Nb. The different mineral assemblages and particularly the compositional trends of tourmaline, dumortierite–holtite and columbite reflect superimposed processes. The initial stage comprises the magmatic crystallization of a highly evolved and boron-rich peraluminous melt. The second stage was a prograde medium-pressure metamorphism, with a fluid-phase-related episode of crystallization. The most likely source of the initial melt is an extraction of residual melt from an almost completely crystallized rare-element parental pegmatite.

Keywords: granitic pegmatite, dumortierite, holtite, chrysoberyl, kyanite, tourmaline, Virorco, Argentina.

§ *E-mail address*: galliski@mendoza-conicet.gov.ar

Introduction

Granitic pegmatites affected by a metamorphic overprint are rather seldom studied, in spite of their great petrological and mineralogical significance. The low abundance of relevant reports may be caused by a tendency to overlook metamorphic features in minerals rather than by the extreme scarcity of such pegmatites in nature. A metamorphic overprint is typical of pegmatites of the abyssal class (Černý & Ercit 2005) described, for example, from Antarctica (Grew 1981, Grew *et al.* 2006, Wadoski *et al.* 2011) or the Bohemian Massif (Losert 1956, Cempírek & Novák 2006, Cempírek *et al.* 2010); these pegmatites are usually located in terranes that underwent multistage metamorphism, and are inferred to have originated through partial melting of metapelites. However, shearing and a metamorphic overprint were reported to have occurred to a variable extent in several rare-element pegmatites as well (*e.g.,* Černý *et al.* 1992, 1994, Němec 1989, Partington *et al.* 1995), causing destabilization of primary assemblages, introduction of Fe-,Mg-,Ti-enriched fluids from host rocks, and recrystallization of phases under new P–T conditions (Černý *et al.* 1992).

In this paper,we re-examined the dumortierite-bearing pegmatites of Virorco, in the San Luis range, Argentina, which were originally described by Gay & Galliski (1978). The pegmatites exhibit signs of metamorphic overprint and deformation typical for abyssal pegmatites, but they also display mineralization that fits well in the rare-element class of granitic pegmatites. The aim of this paper is to communicate the results of a detailed study of the Virorco dikes, including electron-microprobe chemical analyses of minerals, and whole-rock chemical analyses, which were performed in order to clarify their source, origin and paragenetic evolution during their crystallization.

Occurrence

The dikes that we studied are located in the eastern margin of the Virorco River, at latitude 33°05'44"S, longitude 66°07"24"W, and 1284 m of altitude in the San Luis Range, in Argentina (Fig. 1). This area is underlain by feldspathic quartzites, gneisses and migmatites enclosing lenses of norite and hornblende gabbro with minor ultramafic rocks (Pastore & Ruiz Huidobro 1952, González Bonorino 1961). The mafic rocks belong to a NNE–SSW-trending discontinuous belt of mafic–ultramafic rocks; one intrusive body has given a zircon U–Pb age of 478 ± 6 Ma (Sims *et al.* 1997). The host rocks of the mafic–ultramafic belt have undergone granulite-facies metamorphism that gradually decreases over a distance of several kilometers eastward to greenschist facies developed in a thick and strongly folded psammopelitic sequence. The metamorphic rocks were grouped in the Pringles Metamorphic Complex. Zircon crystals in felsic orthogneiss from this complex have yielded metamorphic U–Pb ages of 484 ± 7 Ma, whereas zircon rims in garnet sillimanite gneiss from the complex gave an age of *ca.* 460 Ma (Sims *et al.* 1998). González Bonorino (1961) concluded that the mafic rocks and the metamorphic envelope have both undergone granulite-facies metamorphism, whereas Delpino *et al.* (2007), studying the widespread mylonitic bands that crosscut the metamorphic suites, suggested that mafic rocks and adjacent basement mylonites developed under upper amphibolite transitional to granulite-facies metamorphic conditions at intermediate pressures (668–764°C, 6.3–6.9 kbar, $0.3 < X(CO_2) < 0.7$) during a metamorphic event that involved a counterclockwise P–T path.

The dumortierite-bearing dikes are emplaced in norites and gabbros locally showing widespread development of secondary pargasite, magnesio-cummingtonite and magnesio-hornblende (uralitization). The dikes generally have a thickness between 2 and 3 cm, but locally reach 10 cm; they extend from several decimeters to 1–2 m. The dikes are invariably steeply dipping, commonly striking N60°E, E–W or N–S. Most of the dikes are found as loose broken pieces ~5 to 20 cm in length dispersed on the slope of the hill. The area around the Virorco River is known for other occurrences of pegmatite such as Huemul, a tourmaline-rich, beryl-type rare-element pegmatite that shows evidence of tectonism and crops out approximately 2500 m to the north of the location area of the dumortierite-bearing dikes.

Sampling and Analytical Methods

The present work focused on the dikes 1 to 4 cm thick richest in dumortierite and the most suitable for whole-rock chemical analysis and petrographic research of the complete paragenesis across the dikes. Polished thin sections of the samples were studied with a polarizing microscope prior to carbon-coating for electron-microprobe analysis.

The minerals were analyzed in the wavelength-dispersion mode on a Cameca SX100 electron microprobe of the University of Manitoba, with a beam diameter of 5 μm and an acceleration potential of 15 kV. A sample current of 20 nA measured on a Faraday cup and a counting time of 20 seconds for the element and 10 seconds for the background were used. The standards used were ($K\alpha$ if not specified): albite (Na), apatite (F, P, Ca), olivine (Mg), andalusite (Al, Si), barite (S, Ba$L\beta$), spessartite (Mn), tugtupite (Cl), orthoclase (K), fayalite (Fe), titanite (Ti), VP2O7 (V), chromite (Cr), pentlandite (Ni) and gahnite (Zn).

Other microprobe analyses were performed in the wavelength-dispersion mode using a JEOL JXA–8200 Superprobe of the ETH Zurich, with a beam diameter of 5 μ and an acceleration potential of 15 kV. We used

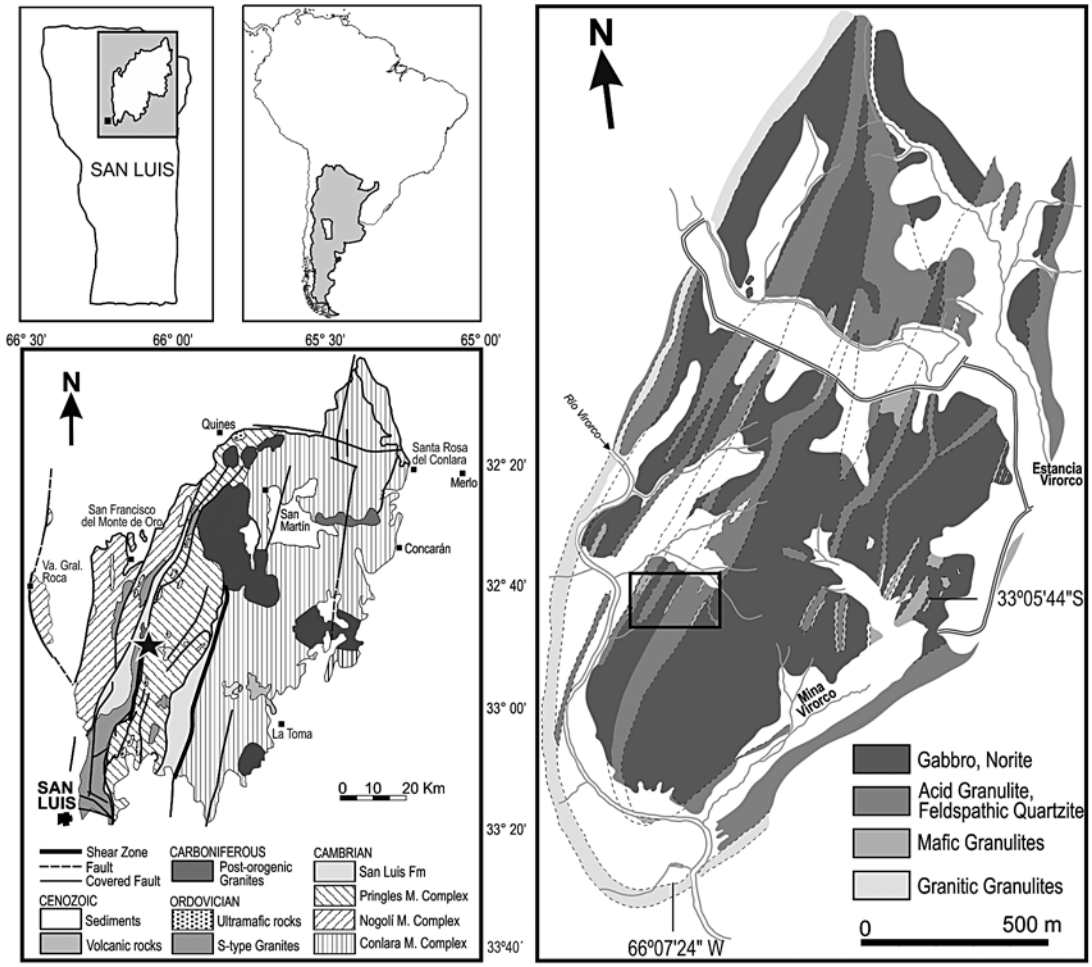

FIG. 1. Location map of the area with dumortierite-bearing dikes in the Virorco Basic Complex, modified from González Bonorino (1961); the star denotes the occurrence of Virorco Basic Complex, and the rectangle outlines the area with dumortierite-bearing dikes.

a sample current of 20 nA measured on a Faraday cup and a counting time of 20 s for the element and 10 s for the background. A combination of silicates and oxides were used as standards for calibration.

The chemical composition of (As–Ta)-rich dumortierite and holtite was studied using an electron microprobe, Cameca SX–100, at the Laboratory of Electron Microscopy and Microanalysis, the joint facility of the Masaryk University and Czech Geological Survey in Brno. The following analytical conditions were applied: acceleration voltage 15 kV, beam diameter 1–5 μm, beam current 10 nA. The standards used were ($K\alpha$ lines if not specified): almandine (Si, Fe), sanidine (Al,K), MgO (Mg), titanite (Ti), spessartine (Mn), topaz (F), lammerite (As$L\alpha$), columbite (Nb$L\alpha$), $CrTa_2O_6$ (Ta$L\alpha$), metallic Sb (Sb$L\alpha$) and Bi (Bi$M\alpha$). For the analysis of tourmaline we added the following standards: albite (Na), grossular (Ca), chromite (Cr), vanadinite (V), benitoite (Ba$L\beta$), NaCl (Cl), gahnite (Zn) and metallic Ni (Ni). Positive correlation of fluorine with Ta and As in dumortierite and surprisingly also with Ta in columbite-tantalite led us to careful examination of EMP standards for a spurious F signal in the presence of As and Ta. The spurious signal was found to correspond to $0.0149*As_2O_3$ and $0.0107*Ta_2O_5$; after correction for As and Ta, the fluorine contents dropped to values below its detection limit.

The data were reduced using the PAP routine of Pouchou & Pichoir (1985). The formulas of tourmaline-supergroup minerals were calculated on the basis of 31

anions using the Excel spreadsheet of J. Selway and Jiang Xiong (2002), where B_2O_3, H_2O and Li_2O are calculated by stoichiometry, assuming B = 3 *apfu*, OH + F = 4 *apfu* and Li = 15 – total($T + Z + Y$). Nomenclature and classification diagrams follow Henry *et al.* (2011).

Whole-rock chemical analysis were performed by Activation Laboratories at Ancaster, Ontario, by FUS–ICP (major elements, Sc, Be, V, Ba, Sr, Y, Zr), FUS–MS (Cr, Co, Ni, Cu, Zn, Ga, As, Rb, Nb, Mo, Ag, In, Sn, Sb, Cs, REE, Hf, Ta, W, Tl, Pb, Bi, Th, U) and PGNAA (B).

TABLE 1. CHEMICAL COMPOSITION OF THE VIRORCO DIKES

Sample	VI01	VI03	VI10	VI11	VI13	VI17
SiO_2 wt.%	74.82	74.49	76.19	72.20	75.09	74.22
TiO_2	0.02	0.01	0.01	0.01	0.01	0.02
B_2O_3	1.03	1.05	1.04	1.09	1.07	1.00
Al_2O_3	17.98	16.73	18.51	17.35	18.70	16.75
FeO	1.37	1.28	0.96	1.73	0.70	2.66
MnO	0.06	0.06	0.36	0.10	0.16	0.07
MgO	0.20	0.23	0.13	0.50	0.13	1.28
CaO	0.80	1.95	0.76	1.54	0.47	1.30
Na_2O	0.60	0.44	1.52	0.32	0.76	1.38
K_2O	0.40	0.04	0.63	0.87	0.35	0.05
P_2O_5	0.42	1.41	0.19	1.08	0.24	0.87
H_2O	0.93	0.72	0.53	1.41	1.38	0.00
Total	98.73	98.90	100.17	98.77	98.88	100.18
B ppm	3040	4350	840	4610	2550	3990
K	3321	332	5230	7222	2905	415
Ba	14	19	50	14	15	30
Rb	287	7	147	523	282	5
Sr	70	103	107	71	46	181
Cs	57.3	12	20.5	94.1	43.8	4.3
Be	224	261	200	187	137	195
Ga	24	21	30	20	29	16
Tl	0.9	0.05	0.5	2.2	0.6	0.02
Ta	278	246	157	436	130	500
Nb	93	77	189	79	75	150
Hf	3.9	4.4	6.2	4.9	2.9	5.5
Zr	47	53	59	32	20	41
Ti	108	78	54	54	30	120
Y	6	9	3	3	1	2
Th	6.9	5.3	5.9	4.6	4	3
U	9	25.2	5.7	11.7	5.6	13.3
Cr	5	10	10	10	10	60
Ni	5	10	10	10	10	40
Co	5	2	2	4	4	5
Sc	0.2	0.05	0.05	1	0.01	2
V	0.2	1	1	5	2	7
Cu	20	10	20	20	50	40
Pb	34	28	19	37	47	26
Zn	15	15	40	40	50	30
As	671	922	50	1060	722	> 2000
Sb	115	>200	6.9	>200	127	> 200
Bi	19.8	27.9	0.8	34.3	15.4	18.5
Sn	64	87	82	55	61	50
W	7	7	3	3	< 1	2
La	6	7.1	2.7	3.3	0.7	3.2
Ce	11.8	14	5.1	5.8	0.7	6.1
Pr	1.24	1.51	0.54	0.62	0.06	0.65
Nd	4.3	5.3	1.8	2.1	0.2	2.2
Sm	0.9	1.1	0.4	0.4	0.05	0.4
Eu	0.05	0.01	0.01	0.01	0.005	0.01
Gd	0.8	1.1	0.3	0.4	0.05	0.4
Tb	0.1	0.2	0.05	0.05	0.05	0.03
Dy	1	1.5	0.4	0.4	0.05	0.04
Ho	0.2	0.3	0.06	0.05	0.05	0.03
Er	0.6	0.9	0.2	0.3	0.05	0.3
Tm	0.09	0.15	0.03	0.02	0.01	0.02
Yb	0.7	1	0.2	0.3	0.05	0.3
Lu	0.1	0.14	0.02	0.04	0.02	0.04

Geochemistry of the Dikes

The chemical analyses were performed on specimens of the dikes selected for showing minimal weathering and variations in intensity of the blue color, which in turn is directly related to the content of tourmaline plus dumortierite, *i.e.*, to the boron content. The results (Table 1) show variable SiO_2 contents (72.2–76.19 wt.%), and very high contents of Al_2O_3 (16.73–18.7 wt.%). The SiO_2 and Al_2O_3 contents are comparable to those of rare-element pegmatites (76.04 and 13.62 wt.% for Tanco; Stilling *et al.* 2006; 69.14 and 14.67 wt.% for Greenbushes, Partington *et al.* 1995) or abyssal pegmatites (~73 and ~15 wt.% for Starkoč vein; Cempírek & Novák 2006), but they differ very significantly from the reported composition of dumortierite-rich kyanite quartzites (Sengupta *et al.* 2011). Values of alumina-saturation index (ASI, the molar ratio Al2O3 / [CaO – $1.67P_2O_5$ + K_2O + Na_2O]; Zen 1986) for the Virorco dikes are very high, in the range 4.27 to 8.52, far beyond the common values of granitic rocks.

The amounts of minor oxides (in wt.%), *i.e.,* MgO (0.13–1.28), FeO (0.70–2.66), and CaO (0.47–1.95) are slightly higher than the average composition at Tanco, possibly due to contamination from the host rock. The MnO contents (0.06–0.36 wt.%) are variable, both lower and higher than at Tanco. The TiO_2 content is low, with values below 0.2 wt.%. Contents of Na_2O (0.32 to 1.52 wt.%) and K_2O (0.04–0.87 wt.%) are very low for a pegmatite. Phosphorus contents of 0.19 to 1.41 wt.% of P_2O_5 vary within the range of values encountered in fractionated rare-element pegmatites or their zones (*cf.* Stilling *et al.* 2006, Partington *et al.* 1995). The boron content, with values ranging from 0.27 to 1.48 wt.% B_2O_3, is very enriched compared to the contents of a classic rare-element pegmatite such as Tanco (0.06 wt.%, Stilling *et al.* 2006), even considering that at Tanco, a significant part of the boron content (>46%) was released to the host rock (Morgan & London 1987).

The whole-rock composition normalized to the upper continental crust shows a depletion in K, Ba, Sr, Zr, Ti, Y, Th, Hf, and Sc. On the other hand, most of the samples provide evidence of enrichment of Rb, Cs, Be, Ta, Nb, U, As, Sb, Sn and B (Fig. 2a). Especially remarkable are the high contents of trace elements typical for the most evolved stages of pegmatite fractionation, such as Cs (4.3–94.1 ppm), Ta (130–500), Be (137–261), and B (840–4610). The REE contents are generally low, in the range of 0.1 to 30 times of average chondrite, and most samples show an enrichment in LREE and a strong negative Eu anomaly (Fig. 2b).

Mineralogy and Petrography of the Dikes

The mineralogy of the dikes is summarized in Table 2. The major minerals of the dikes are quartz, plagioclase, tourmaline-supergroup minerals, dumortierite-group minerals, fluorapatite, muscovite and

kyanite. The accessory and trace minerals include beryl, chrysoberyl, garnet, columbite-group minerals, pollucite, gahnite, thorite, and a few more unidentified minor phases still under study. Staurolite and sillimanite were described by Gay & Galliski (1978), but they were not found *in situ* in the new recently sampled sites.

Most of the pegmatite dikes show, at least in border parts, alignment of prismatic minerals, mostly tourmaline and dumortierite, which are oriented perpendicularly to the contact in the thinner dikes, or under slightly oblique angle in the thicker ones (Figs. 3a, b, c, d, e). In thicker dikes (~5 cm and more), dumortierite is concentrated near the border, whereas in the thinner dikes (2–3 cm), it is abundantly distributed throughout. Both types of dikes show simple symmetrical zonation with border, wall, intermediate and core or central zones; newly formed mineralization was also observed in the dike exocontact.

The host rock of the dike is an altered gabbro with chlorite and relics of hornblende and olivine. In the exocontact of the dikes, the gabbro commonly contains small euhedral and zoned crystals of holmquistite up to at least 1 cm from the contact. Close to the dike border, a fine-grained tourmaline (Tur I) is present as small prismatic crystals pleochroic in shades of brownish green to light brown, together with holmquistite and chlorite.

The fine-grained border zone, up to 3 mm thick along the contact with the host gabbro, is composed of short prismatic euhedral crystals of the dark-colored tourmaline (Tur I) associated with plagioclase, anhedral crystals of fluorapatite and minor quartz (Fig. 3a); the crystals are locally almost perpendicular to the dike border (Figs. 4a, b).

The narrow wall zone (ca. 0.5–1 cm thick) typically consists of anhedral grains of quartz (0.5–2 mm) and subhedral to euhedral prismatic crystals of tourmaline several mm long. At the contact with the border zone, prismatic euhedral crystals of Tur I were found overgrown by anhedral (Fe–Mg)-rich Tur II and elbaite–rossmanite tourmaline III and IV (Fig. 4a). Farther from the border zone, the tourmaline typically has a colorless core of elbaite–rossmanite (Tur III and IV) and a dark blue anhedral Fe-rich rim (Tur V) with abundant inclusions of quartz (Fig. 4b). Tourmaline III and IV are usually partially or completely replaced by tourmaline V; their contact is gradational, and in some cases, Tur III and IV form only small patches in Tur V (Fig. 4c). The tourmaline V usually encloses the tourmaline III and IV in a form of skeletal grains intergrown with quartz, or more commonly, as anhedral irregular patchily-zoned overgrowths with diffusive contacts with tourmaline III or IV; the textures are typical of fluid-driven dissolution-reprecipitation of tourmaline during a prograde stage of metamorphic overprint (*cf.* Fig. 4 in Kalt *et al.* 2001, Fig. 6 in Henry *et al.* 2002, Fig. 3 in Marschall *et al.* 2008). The Tur V is commonly intergrown or replaced by aggregates of quartz and pleochroic (colorless to blue) needles of dumortierite (Dum I, Fig. 4d). Abundant small inclusions of pollucite are present in the relics of the tourmaline III and IV in the wall zone (Fig. 4c). Locally, the wall zone contains relics of albite crystals replaced by oligoclase and quartz; the replacement is also associated with dumortierite I overgrowths on tourmaline V, the presence of kyanite, and rare anhedral grains of chrysoberyl.

The intermediate zone constitutes volumetrically most of the dikes, and it is largely composed of light-colored minerals like quartz, plagioclase, muscovite, tourmaline, beryl, chrysoberyl, kyanite, and dumortierite-group minerals, as well as rare columbite-tantalite. Quartz is usually medium-grained; in thin dikes, larger anhedral quartz grains are commonly rimmed by a

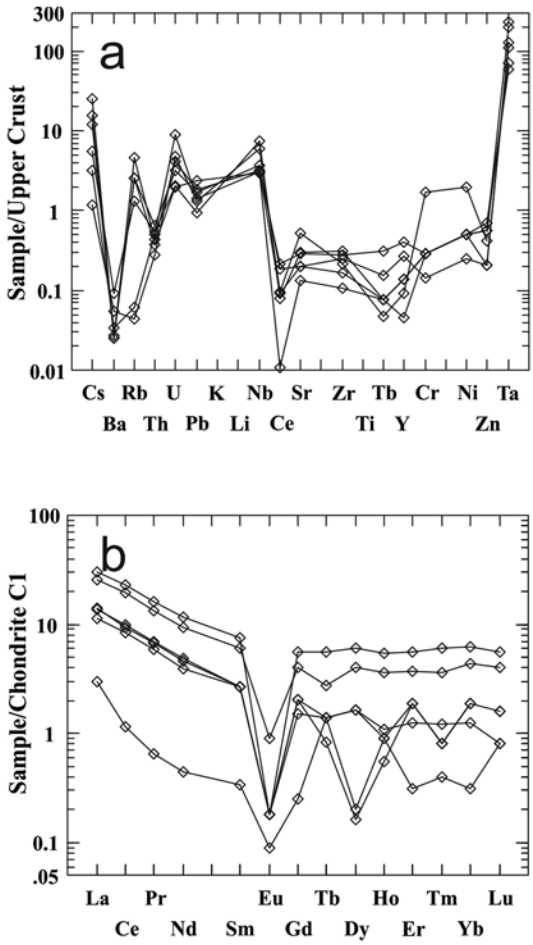

FIG. 2. a. Spider diagram showing the samples of the Virorco pegmatites normalized to the average upper continental crust (Taylor & McLennan 1995); b: rare-earth element contents of the Virorco pegmatites (normalized to CI chondrite, McDonough & Sun 1995).

TABLE 2. MINERALOGY OF THE VIRORCO PEGMATITES

Sample	VI01	VI02	VI03	VI04	VI05	VI06	VI07	VI08	VI09	VI10	VI11	VI12	VI13	VI14	VI15	VI16	VI17
Thickness	2.3	2.5	1.6	3.8	3.0	4.8	4	2	4.1	3.6	1.3	3.9	2.4	3	1.9	2.5	1.2
WR Anal.	●		●							●	●		●				●
EPMA		●	●	●		●			●	●			●	●	●		●
Quartz	X	X	X	X	X	X	X	X	X	X	X	X	X	X	X	X	X
Tourmaline	X	X	X	X	X	X	X	X	X	A	X	X	X	X	X	X	X
Dumortierite	X	X	X	X	X	X	X	A	A	X	X	X	X	X	X	X	X
Holtite	A		A	A	A		T		A	A	A	A	A	A	A		X
Muscovite			T	X	A	T	T	T	X	A	X	A		X		X	
Plagioclase	A	A		X			A	A	X	A	A	X		A	A	X	A
Kyanite	T	X		A	X		X	X		X	X	X	T	A	A	X	
Beryl	A	A	T	A		T			A							A	
Chrysoberyl		A	T			T	A						T	A		A	
Garnet				A		T	A			T		A		A		A	A
Apatite group		A	T							T	A		T	A			
K-feldspar		T			T		T	A		A	T	T	A	T	T	T	T
Pollucite			T														
Columbite-(Mn)				T		T							T		T		
Tantalite-(Mn)						T							T		T		
Bismuth	T																
Rutile					T												
Zircon										T							
Gahnite			T											T			
Amphibole								T						T			

X: abundant, A: scarce, T: traces. Thickness is quoted in cm. WR anal.: whole-rock analysis, EPMA: electron-probe micro-analysis.

fine-grained assemblage of plagioclase, quartz and fluorapatite with coarse grains of kyanite, fine crystals and sprays of dumortierite, and relics of tourmaline V. In thicker dikes, plagioclase forms laths showing polysythetic twinning, but in thin dikes, a fine-grained Ca-rich plagioclase is common. In thicker dikes, primary muscovite is present in thick crystals of dull pink color, up to 5 mm long; along the contact with the fine-grained plagioclase assemblage, it is usually rimmed by muscovite + quartz symplectite. Muscovite crystals are commonly replaced by dumortierite I along cleavage planes. Tourmaline in the intermediate zone is represented by euhedral crystals of the elbaite–rossmanite, tourmaline III and IV; where it is in contact with the fine-grained assemblage, the tourmaline is replaced by a symplectite of quartz and Fe-rich tourmaline V, followed by a symplectite of quartz and dumortierite I and II. Beryl was rarely observed in subhedral grains and prisms up to 1 cm long; it locally contains tiny inclusions of pollucite, and on grain rims it is commonly replaced by anhedral chrysoberyl and quartz. In several dikes, a macroscopically blue or greenish brown core or central zone rich in dumortierite-group minerals, fluorapatite and fine-grained plagioclase can be recognized.

Lensoidal aggregates composed of dumortierite in prismatic or acicular crystals or bundles of fibers a few millimeters across are widespread in the Virorco dikes. The prismatic crystals are found mostly in the intermediate zones, but in the thicker dikes, they occur in some cases in the wall zones. In the central part of the dikes, dumortierite is common in distorted bundles of fibers. The color is usually light to deep blue with some brownish tinge in the fibrous aggregates. Four textural and compositional types of dumortierite-group minerals were recognized in the dikes. Dumortierite I (Dum I) is the earliest and the most common dumortierite phase in the dikes. Dum I together with quartz usually overgrow and partially or completely replace tourmaline III and IV (Figs. 5b, c), kyanite, and in the central zone, it replaces muscovite along cleavage planes. In turn, it is replaced by holtite and, in some cases, by kyanite. Dumortierite II forms sector-zoned crystals that are commonly overgrown by zones of dumortierite III + holtite. Holtite occurs in some dikes, especially in the thinner ones that are richest in dumortierite and consequently the most boron-rich. It occurs as bundles of needle-like crystals that commonly show cyclic twinning. Its color is green in polished surfaces

FIG. 3. a–e. Polished sections of the most representative dumortierite-bearing dikes showing the different textural arrangements; scale bar is 1 cm. f–j. Photomicrographs of selected minerals, scale bar is 200 μm. f. Pale yellow to brownish yellow acicular and prismatic crystals of holtite (Hol) growing within bundles of dumortierite. g. Tabular colorless crystals of chrysoberyl (Chr) nestled in dumortierite. h. Bundles of blue dumortierite (Dum). i. Kyanite (Ky) associated with, and in part replacing, blue dumortierite. j. Kyanite intercalated and replacing muscovite (Ms), and associated with dumortierite.

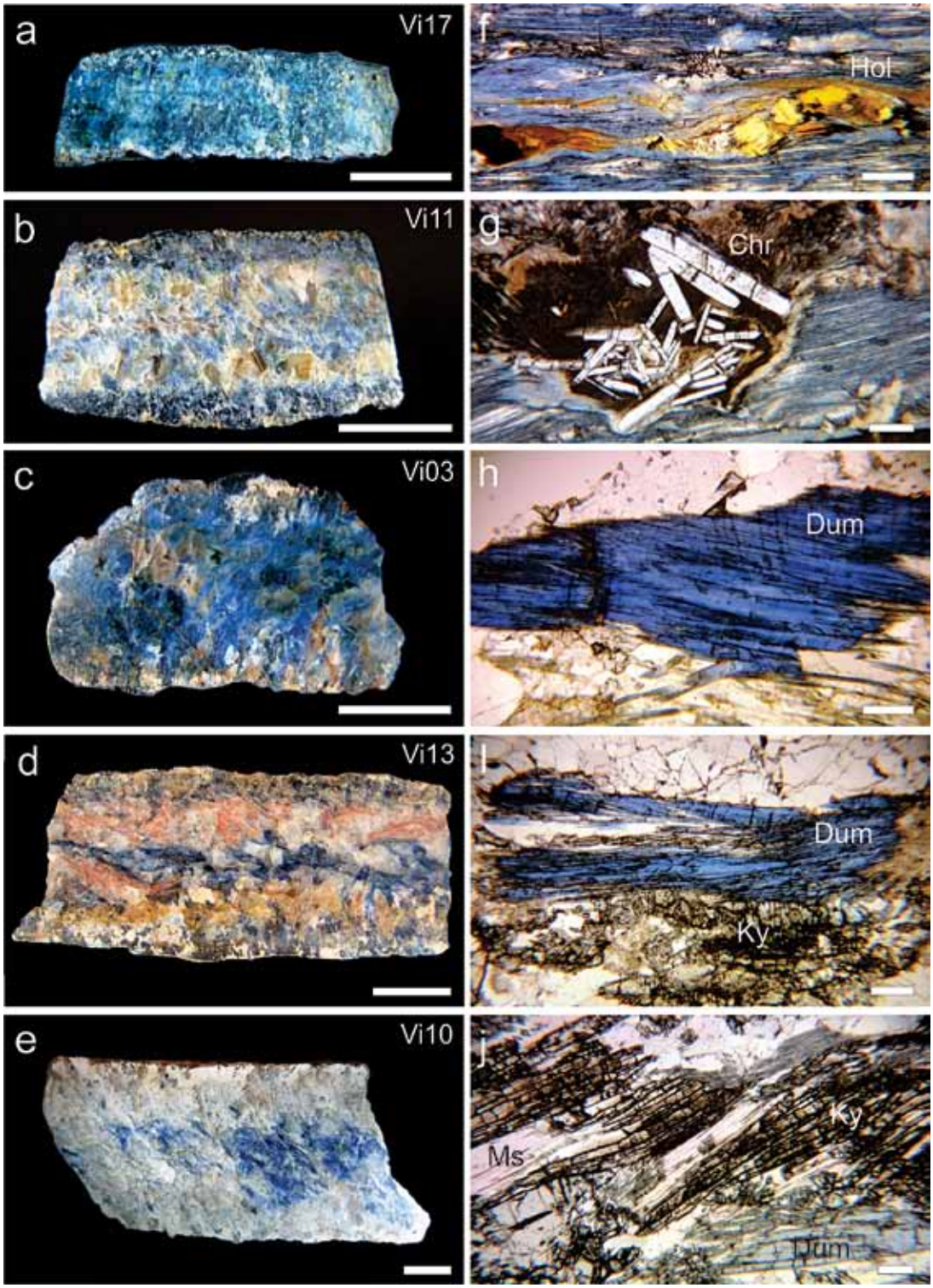
a
Vi17
b
Vi11
c
Vi03
d
Vi13
e
Vi10
f
Hol
g
Chr
h
Dum
i
Dum
Ky
j
Ky
Ms
Dum

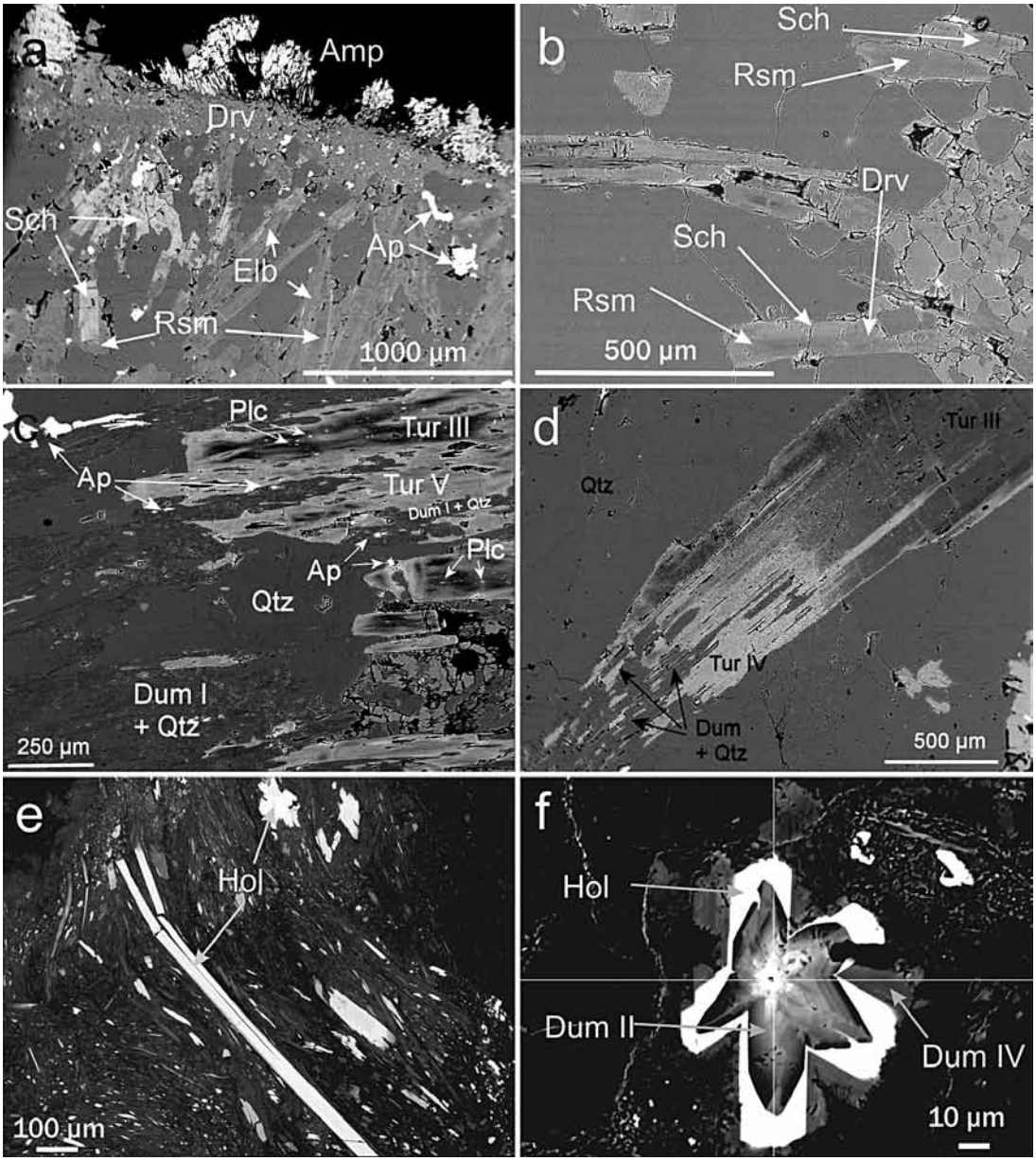

FIG. 4. Back-scattered electron images of the most significant minerals from the dumortierite-bearing dikes. a. Contact between amphiboles in the norite host-rock and a dumortierite-bearing dike; note the development of border and wall zone and the zoning in tourmaline. b. Detail of the tourmaline zoning from the border zone (to the right) inward. c. Zoned crystals of tourmaline, which is partially replaced by dumortierite. Tourmaline encloses tiny grains of pollucite. d. Zoned crystal of tourmaline with the tip replaced by dumortierite plus quartz. e. Broken acicular crystal of holtite included in dumortierite. f. Basal section of the cyclic twins of a composite dumortierite–holtite crystal showing radial zoning.

of hand specimens, but pleochroic from greenish yellow to yellowish brown under the microscope. Holtite commonly is associated with dumortierite, showing in a very short distance a color change from deep blue to a brownish transition zone and then to a greenish yellow color. Holtite is locally in contact with an ore mineral that has largely broken down, leaving some darker spots, possibly columbite (Fig. 3f). Back-scattered electron images of holtite show that the fibers are in many cases broken (Fig. 4e), and that the basal sections of cyclic twins show zoning, with dumortierite-dominant central parts that pass outward to holtite-dominant overgrowths (Figs. 4f, 5a). Holtite also forms individual crystals usually overgrown by dumortierite IV. All dumortierite types were found embedded in oligoclase, quartz or fluorapatite, and rarely were found enclosed in skeletal grains of spessartine (Fig. 6d).

Kyanite is abundant in most of the dikes, especially in those poorer in boron, where it usually occurs together with dumortierite. It forms long prismatic to tabular twinned crystals with sharp terminations in clusters of two to three individuals. Both cases, kyanite being replaced by dumortierite I, as well as kyanite replacing dumortierite I and muscovite, were observed (Figs. 3i, 3j).

Among the accessory phases, beryl occurs in a few dikes, rarely associated with chrysoberyl. It usually forms anhedral to subhedral isolated crystals, very rich in crystallographically oriented inclusions, enclosed in quartz in the intermediate zones. Chrysoberyl is more common and, typically forms small tabular crystals up to 0.5 mm long (Fig. 3g) grouped without preferred orientation and nestled in bundles of fibers of dumortierite or holtite. Much rarer are anhedral grains enclosed in quartz and associated with or enclosed in anhedral grains of beryl. The microstructure illustrated in Figure 6e suggests that some chrysoberyl could have formed from breakdown of beryl by one of two reactions: beryl → chrysoberyl + 3 quartz +2 BeO (Černý *et al.* 1992) or beryl + 2 aluminosilicate → 3 chrysoberyl + 8 quartz (Franz & Morteani 2002). Cracks in brecciated chrysoberyl are filled with Dum II and Dum III + holtite (Fig. 6f).

Anhedral grains of metamict zircon with common inclusions of uraninite are relatively frequent in the assemblage of oligoclase, fluorapatite, kyanite and dumortierite in several samples. The zircon grains are 10–200 μm across; spot analyses yielded the formula $(Zr_{0.91}Hf_{0.08})SiO_4$ with trace contents of uranium. Metamict thorite was observed as rare inclusions in fluorapatite.

Some dikes show evidence of deformation, either across their entire thickness or only in their central parts, and ranging from incipient to strong. This deformation is usually pronounced and led to bending or breakage of prismatic minerals (*e.g.,* tourmaline, kyanite), muscovite sheets and plagioclase; it is exceptionally well developed in dumortierite and holtite, especially in the varieties that form bundles of fibrous crystals. The deformation occurs during the crystallization of the different generations of dumortierite, as is shown by the bent and broken prisms. In extreme cases of

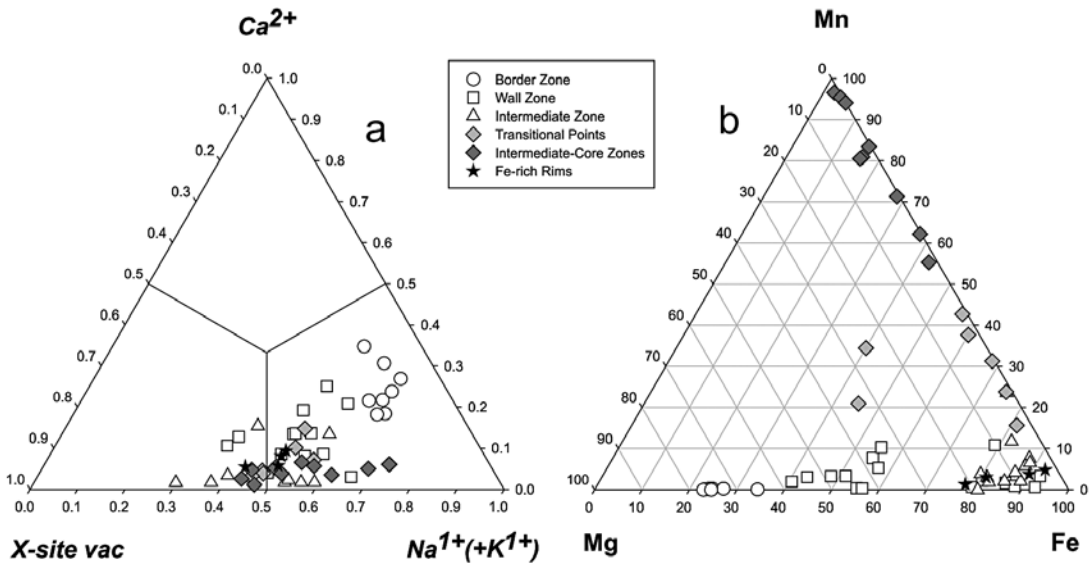

FIG. 5. a. *X*-site chemical composition of the tourmaline from Virorco dikes. b. Contents of Fe^{2+}, Mn, Mg in ($Y + Z$) sites of the tourmaline.

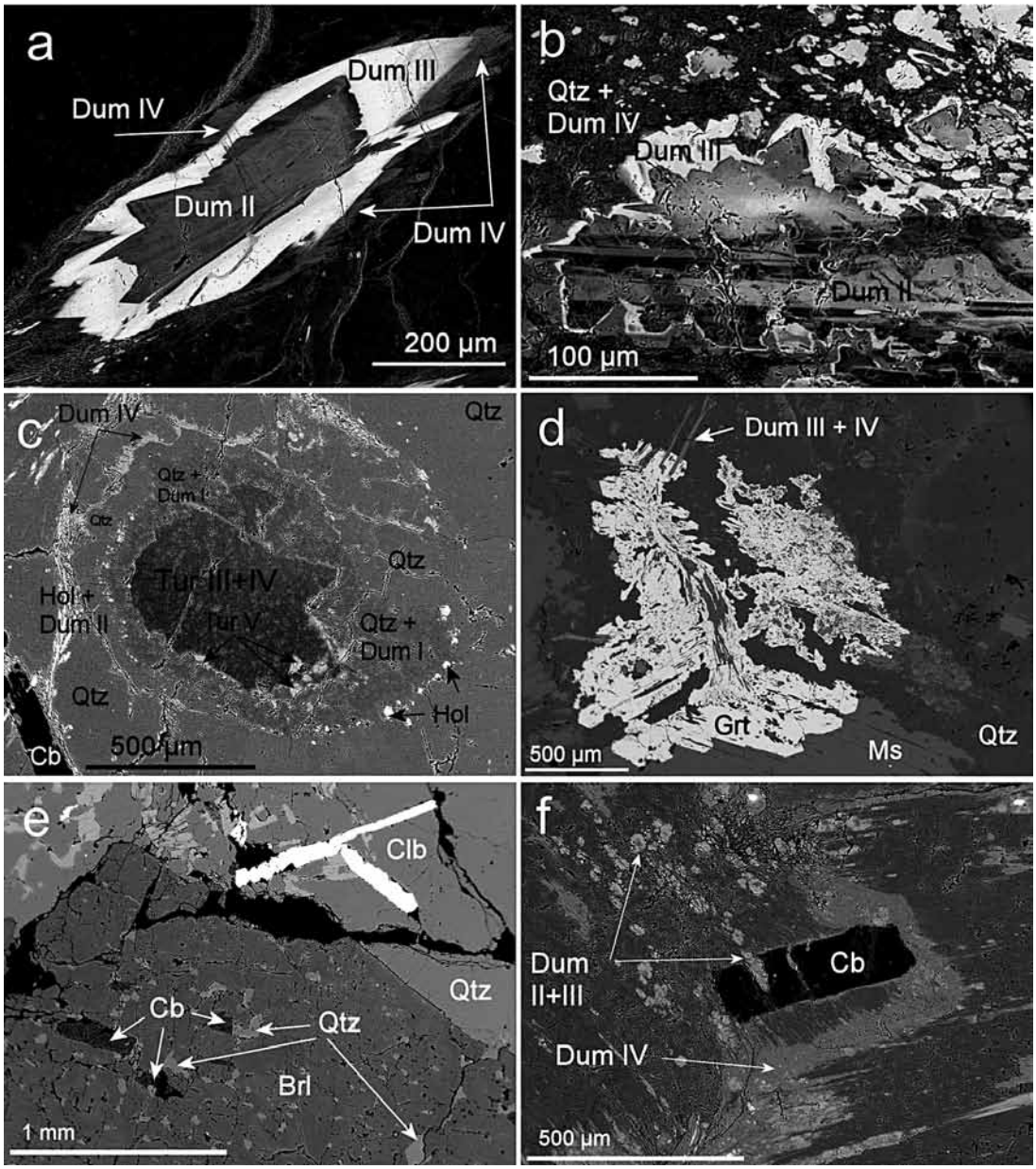

FIG. 6. BSE images of the most significant minerals. a. Oblique section of a prismatic crystal of a dumortierite-group mineral (Dum) showing the last three of four generations recognized. b. Sequence of different crystals of dumortierite (Dum). c. Tourmaline replaced by dumortierite + quartz. d. Skeletal crystal of spessartine including dumortierite III. e. Anhedral crystal of beryl showing incipient breakdown to chrysoberyl + quartz; to the right are tabular crystals of columbite-(Mn). f. Fractured tabular crystal of chrysoberyl partially replaced by dumortierite II + III (holtite), and surrounded by dumortierite IV.

deformation, some dikes show complete recrystallization of the minerals in different domains. Some show large secondary crystals of quartz with a mortar texture in the borders, or a few areas that concentrate small tabular crystals of plagioclase, and lensoid aggregates composed mostly of dumortierite, holtite and kyanite in small prismatic or asbestiform crystals.

Signs of fluid exchange between the host rock and the dikes are widespread, *i.e.,* oligoclase replacing the primary albite, or Fe-rich tourmaline (Tur V) replacing primary elbaite–rossmannite (Tur III and IV). Texturally unambiguous proof of mass exchange was provided by a single sample (V105) in which a small xenolith of the host rock is trapped in the pegmatite dike; the mass of the xenolith is now composed predominantly of tourmaline (zoned crystals of dravite–schorl) and fluorapatite, whereas in the dike, decreasing amount of Fe-rich tourmaline V replacing tourmaline III and IV is clearly visible in a direction away from the xenolith.

Chemical Composition of the Minerals

Plagioclase

Plagioclase occurs in at least two generations. Primary albite (Ab_{98-99}) forms subhedral crystals that show polysynthetic twinning. It occurs intergrown with tourmaline in the wall zone of several dikes, and normally with undulose extinction and bending of twin planes. From the grain borders inward, it is usually replaced by oligoclase ($An_{15.7–27.3}Ab_{72.3–83.7}Or_{0.4–0.6}$), forming fine-grained aggregates associated with abundant fluorapatite, kyanite, tourmaline V and dumortierite-group minerals. Myrmekite is found in a few samples. Plagioclase is lightly altered to fine-grained white mica in most dikes.

Tourmaline

Tourmaline of the Virorco pegmatites belongs to the alkali- and *X*-vacant groups (Figs. 5a, b, Table 3). It shows a remarkable compositional variation from the dike exocontact and border zone to the core zone. From the host rock inward, the dravite Tur I in the exocontact and the border zone features the highest contents of Ca (0.135 – 0.341 *apfu*), Ti (up to 0.06 *apfu*) and Mg (1.111–2.274 *apfu*), and slightly lower content of Al between ~5.6 and 6 *apfu*, suggesting the presence of a uvite component in the predominant dravite. The Tur II in the wall zone shows a gradual increase of Fe/(Fe + Mg + Mn) from 0.40 to 0.93, an increase in Al contents from 6.3 to 7.6 *apfu*, and a decrease in contents of Ca. The elbaite (Tur III) and rossmanite (Tur IV) from wall, intermediate and core zones of the dikes, feature abrupt change to Al-, Li- and Mn-rich compositions, with up to 4.05% MnO (Fig. 6b). The gradational boundary between Tur II and III and Fe-rich tourmaline (Tur V) results in compositions intermediate between Mn-rich elbaite–rossmanite and Al-rich schorl, with a variable Fe/Mn ratio. The "pure" tourmaline V shows high amounts of Al and considerable *X*-site vacancy, intermediate between Al-rich schorl and foitite (Fig. 5a). The chemical composition and assemblages of tourmaline in Virorco pegmatites illustrate well that tourmaline is sensitive to changes in the crystallization parameters and bulk composition of the system (*e.g.,* van Hinsberg *et al.* 2011, and references therein). The tourmaline compositions and textures in the three main zones of the Virorco dikes are very distinct; the bases of the prisms consist of tourmaline III. They pass to light tourmaline IV in the crystal centers, being Mn-rich elbaite with a gradual transition to rossmanite that ends with Fe-rich tourmaline V in the rims. In the wall zone, the Mn-rich tourmaline IV locally forms patches (dark in BSE image) with rare inclusions of pollucite or gahnite (Fig. 4c). In the dike center, the tourmaline IV forms euhedral prismatic crystals. The Fe-rich tourmaline V usually encloses the tourmaline IV in a form of skeletal grains intergrown with quartz, or more commonly, as anhedral irregularly patchy-zoned overgrowths with diffusive contacts with tourmaline IV. The tourmaline V is commonly overgrown or partially replaced by blue dumortierite (Fig. 4d); replacement of dravite by dumortierite was not observed. An exceptional sequence was found locally in the wall zone, where the schorl cores of some prismatic crystals grade in to rossmanite (Fig. 4a). In this case, the sequence of formation is dravite → schorl → rossmanite.

Dumortierite – Holtite

The composition of dumortierite-group minerals ranges from almost pure dumortierite with formula $\sim(Al,\square)Al_6(BO_3)Si_3O_{16}(O,OH)_2$ to Ta- or As-rich holtite (Table 4, Fig. 7). Whereas dumortierite II shows a good 3:2:1 correlation in its contents of (Ta + Nb), (As + Sb + Bi) and (Fe + Mg), respectively, the decrease in (Ta + Nb) seems to be independent on the strong increase in (As + Sb + Bi) in the dumortierite III (Dum III), and in Dum IV, the high contents of (As + Sb + Bi) are present at very low contents of (Ta + Nb). The data clearly show that the incorporation of Ta is independent of incorporation of As + Sb + Bi, *i.e.,* they are not involved in a coupled stubstitution (*e.g.,* Hoskins *et al.* 1989), and that several different substitutions are involved.

Among the substituents at the partially occupied octahedral Al(1) site, Ta, Nb, Ti and Fe are the most common. Enrichment of Ta from Nb is most obvious in Dum II (Fig. 8a) as crystallization proceeds. In Dum III, however, Nb increases with (As + Sb + Bi) contents. Arsenic and Sb are the main substituents for Si at tetrahedral sites in Dum II and III; Dum I and IV exhibit very low Sb contents. Arsenic does not exhibit

TABLE 3. SELECTED COMPOSITIONS OF TOURMALINE-SUPERGROUP MINERALS

Sample	Vi15	Vi15	Vi115	Vi14	Vi14	Vi14	Vi04	Vi03	Vi03	Vi13	Vi13	Vi13
Point	117	118	119	62	63	64	34	11	10	17	18	19
Mineral	Drv	Drv	Drv	Srl	Srl	Srl	Rsm	Rsm	Rsm	Elb	Elb	F-Elb
SiO_2 wt.%	37.25	36.68	37.73	33.71	33.66	34.60	34.40	36.20	35.25	34.07	37.86	37.53
TiO_2	0.14	0.24	0.37	0.00	0.05	0.02	0.02	0.00	0.01	0.02	0.00	0.00
Al_2O_3	30.10	30.41	30.03	33.50	32.88	33.12	44.56	38.90	42.55	40.23	40.76	40.44
V_2O_3	0.00	0.00	0.00	0.00	0.00	0.00	0.00	0.00	0.01	0.00	0.00	0.00
Cr_2O_3	0.90	0.28	0.17	0.00	0.00	0.00	0.04	0.10	0.00	0.00	0.01	0.01
FeO	5.09	5.16	5.13	14.65	13.88	15.26	0.87	8.50	6.04	6.10	0.20	0.29
MgO	8.66	9.18	9.10	1.02	1.97	0.63	0.01	1.00	0.24	0.06	0.01	0.00
CaO	1.24	1.35	1.05	0.73	1.36	0.47	0.28	0.10	0.16	0.84	0.30	0.36
MnO	0.05	0.03	0.04	0.15	0.11	0.10	2.18	0.40	0.39	1.91	4.46	4.54
ZnO	0.00	0.00	0.00	0.04	0.09	0.03	0.15	0.00	0.04	0.00	0.00	0.00
BaO	0.01	0.00	0.07	0.00	0.06	0.05	0.01	0.00	0.00	0.00	0.00	0.00
Na_2O	2.00	2.02	2.07	1.46	1.50	1.73	1.44	1.20	1.47	1.59	2.27	2.38
K_2O	0.02	0.02	0.03	0.03	0.02	0.03	0.01	0.00	0.01	0.04	0.03	0.04
F	0.20	0.21	0.41	0.11	0.03	0.04	0.08	0.00	0.05	0.42	0.93	1.10
Cl	0.01	0.00	0.00	0.01	0.01	0.01	0.00	0.00	0.00	0.01	0.00	0.01
H_2O*	3.58	3.56	3.51	3.45	3.50	3.51	3.74	3.74	3.77	3.48	3.42	3.31
B_2O_3*	10.67	10.61	10.73	10.14	10.18	10.23	10.96	10.83	10.99	10.67	11.18	11.12
Li_2O*	0.43	0.17	0.47	0.11	0.18	0.21	1.23	0.61	0.92	0.95	1.65	1.65
Total	100.35	99.93	100.91	99.11	99.48	100.04	99.99	101.58	101.90	100.40	103.07	102.70
O=F	0.08	0.09	0.17	0.05	0.01	0.02	0.03	0.00	0.02	0.18	0.39	0.46
Total*	100.26	99.84	100.74	99.06	99.47	100.02	99.95	101.58	101.88	100.22	102.68	102.32
T: Si	6.070	6.007	6.109	5.775	5.745	5.877	5.454	5.808	5.573	5.547	5.885	5.868
Al	0	0	0	0.225	0.255	0.123	0.546	0.192	0.427	0.453	0.115	0.132
B	3	3	3	3	3	3	3	3	3	3	3	3
Z: Al	5.781	5.870	5.730	6	6	6	6	6	6	6	6	6
Mg	0.219	0.130	0.270	0	0	0	0	0	0	0	0	0
Cr	0	0	0	0	0	0	0	0	0	0	0	0
Y: Al	0	0	0	0.539	0.360	0.508	1.78	1.163	1.501	1.267	1.353	1.320
Ti	0.017	0.03	0.045	0	0.010	0	0	0	0	0	0	0
V	0	0	0	0	0	0	0	0	0	0	0	0
Cr	0.116	0.036	0.022	0	0	0	0.010	0.013	0	0	0	0
Mg	1.885	2.111	1.927	0.261	0.501	0.16	0	0.239	0.057	0.015	0	0
Mn	0.01	0	0.010	0.022	0.016	0.014	0.293	0.054	0.052	0.263	0.587	0.601
Fe^{2+}	0.694	0.707	0.695	2.099	1.981	2.168	0.115	1.140	0.799	0.831	0.026	0.040
Zn	0	0	0	0.010	0.011	0	0.018	0	0.010	0	0	0
Li*	0.282	0.113	0.306	0.074	0.124	0.144	0.785	0.391	0.584	0.622	1.03	1.039
Sum *Y*	3	3	3	3	3	3	3	3	3	3	3	3
X: Ca	0.216	0.237	0.182	0.134	0.249	0.086	0.048	0.017	0.027	0.147	0.050	0.060
Ba	0	0	0	0	0	0	0	0	0	0	0	0
Na	0.632	0.641	0.650	0.485	0.496	0.570	0.443	0.373	0.451	0.502	0.684	0.722
K	0	0	0.010	0.010	0	0.010	0	0	0	0.010	0.010	0
X-site vacancy	0.147	0.118	0.157	0.374	0.247	0.335	0.507	0.610	0.520	0.343	0.260	0.210
OH	3.894	3.891	3.790	3.937	3.981	3.976	3.960	4	3.975	3.781	3.543	3.453
F	0.103	0.109	0.210	0.060	0.016	0.021	0.040	0	0.025	0.216	0.457	0.544
Cl	0	0	0	0	0	0	0	0	0	0	0	0

Symbols: Drv: dravite, Elb: elbaite, F-Elb: “fluor-elbaite”, Rsm: rossmanite, Srl: schorl.

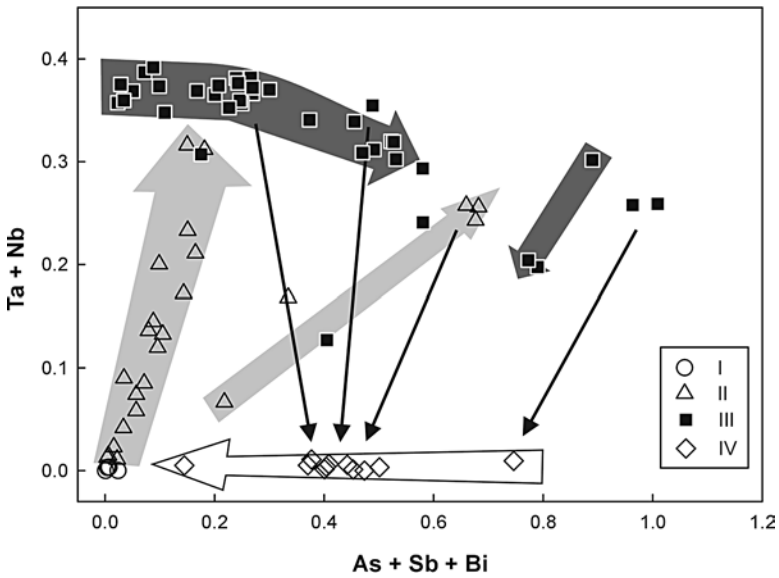

FIG. 7. Plot of Ta + Nb *versus* As + Sb + Bi *apfu* showing the different generations (I, II, III, IV) of dumortierite–holtite minerals from the Virorco pegmatitic dikes.

strong enrichment over Sb unless contents of As reach ~0.3 *apfu* (Fig. 8b); above this value, the content of As rises to 0.9 *apfu*, whereas Sb remains relatively constant at ~0.07 *apfu*. Contents of Fe increase in Dum II, and drop abruptly in Dum III with increase of As + Sb + Bi (Fig. 8c). Minor amounts of P (~0.1 *apfu*) show a positive correlation with As + Sb + Bi contents (Fig. 8d).

Columbite-group minerals

Minerals of the columbite-group are rarely present in traces as small (~50 μm) tabular zoned crystals (Fig. 6e) with columbite-(Mn) in the core and tantalite-(Mn) at the rim (Table 5). They were found in the intermediate zone, together with beryl and chrysoberyl. These crystals show minor replacement of tantalite-(Mn) with material having a Ta/(Ta + Nb) value in the range of values of primary columbite but at slightly higher Fe contents (Fig. 9).

Whereas the rimward increase of Ta/(Ta + Nb) in columbite-tantalite is a regular feature of magmatic fractionation in granitic rocks, the very high Mn/(Fe + Mn) is rather unusual and typical especially of highly fractionated pegmatites; it suggests that the primary assemblages in Virorco originated from a highly fractionated melt.

Beryl and chrysoberyl

The chemical composition of beryl shows a slightly elevated amount of alkalis (Table 6), especially Na (≤0.29 wt.% Na_2O; 0.051 *apfu* Na) and Cs (≤0.48 wt.% Cs_2O; 0.018 *apfu* Cs). The amount of Cs is comparable to that from less fractionated rare-element pegmatites (*e.g.*, Trueman & Černý 1982). Chrysoberyl has a rather homogeneous stoichiometric composition, with trace amounts of Fe (≤0.18 wt.% Fe_2O_3). Higher contents of Fe, between 0.77 and 1.44 wt.% Fe_2O_3 (0.024–0.047 *apfu* Fe^{3+}) were encountered in sample Vi02.

Kyanite

The chemical composition of kyanite is close to the ideal formula; interestingly, it features elevated contents of Fe between 0.3 and 0.73 wt.% Fe_2O_3. These contents are even higher to those reported in kyanite from metamorphic rocks, but lower than in kyanite from high $f(O_2)$ environments (Deer *et al.* 1997).

Muscovite

Muscovite occurs in scarce, tabular, locally crumpled dull pinkish crystals. Its composition is variable but normally Na-rich ($K_{1.181–1.611}$, $Na_{0.411–0.294}$) (Table 7). Lithium was not sought, but the electron-microprobe data do not significantly deviate from the regular muscovite–paragonite solid-solution. The elevated paragonite component (17–26 mol.%) is comparable to that in muscovite from less fractionated rare-element pegmatites (*e.g.*, Alfonso *et al.* 2003, Vieira *et al.* 2011). Muscovite is commonly replaced by dumortierite I and also by kyanite.

Garnet

Garnet is a common accessory phase in small quantities. It is anhedral to subhedral, and commonly overgrows all generations of dumortierite and holtite (Fig. 5D). Its composition ($Sps_{68.8–95.6}Alm_{2.5–26.5}Adr_{0–2}Grs_{tr}Uv_{tr}$) is variable along the spessartine–almandine solid solution, with spessartine as the dominant component (Table 8).

Gahnite

A single analysis of a small grain of gahnite provided data with reasonable sum of oxides (98.94 wt.%) and formula $(Zn_{0.95}Fe_{0.02}Mn_{0.02})Al_2O_4$.

Discussion

The mineralogical assemblage of the Virorco dikes shows the superposition of more than one paragenesis in response to changing conditions. To understand these successive stages, it is necessary to examine each indi-

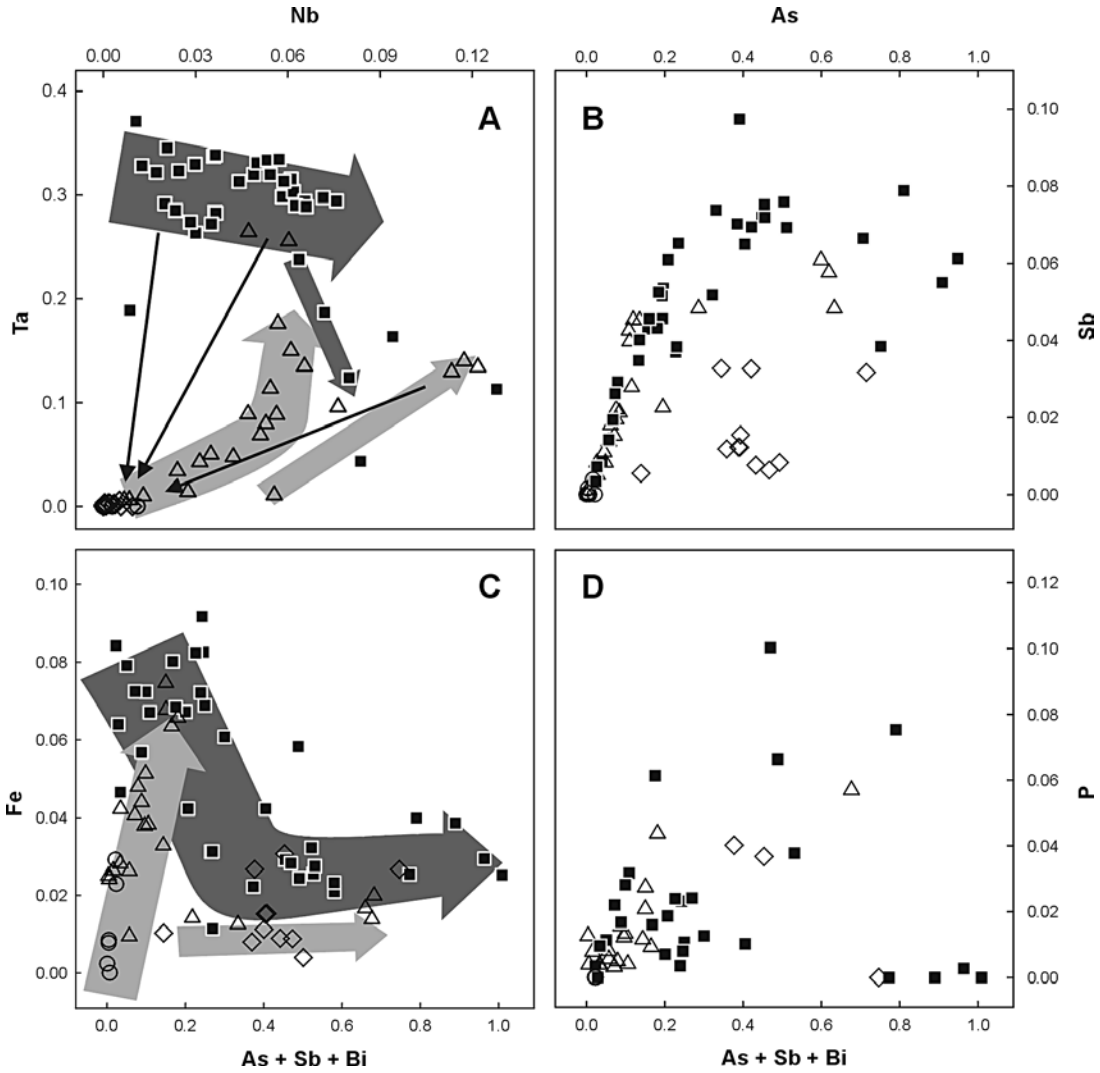

Fig. 8. Variation diagrams of dumortierite–holtite from the Virorco pegmatitic dikes, expressed in *apfu*; symbols I, II, III, IV represent the different generations of dumortierite. a: Nb *versus* Ta, b. As *versus* Sb. c. As + Sb + Bi *versus* Fe. d. As + Sb + Bi *versus* P.

TABLE 4. REPRESENTATIVE COMPOSITIONS OF DUMORTIERITE-GROUP MINERALS

Sample	106	113	113	113	113	113	113	113	106	106	113	3	3	113	113
Anal. #	41	89	71	68	70	67	78	79	3	4	46	23	24	82	83
Type	I		II				III							IV	
Ta_2O_5 wt.%	0.00	0.00	1.98	3.09	5.67	9.67	11.47	11.21	10.01	4.09	6.75	5.64	6.39	0.04	0.21
Nb_2O_3	0.00	0.00	0.82	1.21	1.36	1.01	1.13	1.23	0.75	2.72	0.18	1.95	1.48	0.00	0.13
P_2O_5	0.00	0.00	0.04	0.05	0.10	0.49	0.20	0.26	0.00	0.00	0.83	0.03	0.00	0.45	0.49
TiO_2	0.00	0.00	0.00	0.01	0.02	0.04	0.00	0.00	0.00	0.00	0.01	0.01	0.14	0.00	0.00
SiO_2	31.15	29.84	29.19	28.06	26.64	25.42	25.63	25.09	22.35	21.99	20.25	19.40	18.70	25.70	26.16
As_2O_3	0.01	0.38	0.98	1.42	1.95	2.13	2.45	3.19	6.77	7.99	11.53	14.01	14.51	7.17	5.86
Sb_2O_3	0.00	0.00	0.36	0.54	1.11	1.07	1.05	1.40	1.63	1.62	0.88	1.25	1.38	0.84	0.84
Bi_2O_3	0.01	0.08	0.03	0.00	0.00	0.02	0.06	0.00	0.09	0.00	0.00	0.00	0.00	0.00	0.00
Al_2O_3	62.06	61.80	59.75	58.04	55.30	52.01	50.06	50.06	49.92	52.75	50.95	51.04	50.76	59.08	59.03
B_2O_3	6.20	6.14	6.07	5.95	5.78	5.58	5.48	5.47	5.43	5.60	5.53	5.60	5.56	6.06	6.03
FeO	0.03	0.29	0.51	0.47	0.75	0.74	0.47	0.12	0.35	0.24	0.44	0.33	0.28	0.38	0.33
MnO	0.00	0.00	0.01	0.03	0.03	0.04	0.01	0.02	0.06	0.07	0.01	0.00	0.00	0.02	0.02
MgO	0.01	0.09	0.03	0.01	0.02	0.00	0.00	0.00	0.00	0.00	0.00	0.00	0.00	0.00	0.00
K_2O	0.01	0.02	0.00	0.01	0.00	0.00	0.02	0.01	0.00	0.00	0.00	0.02	0.00	0.00	0.01
F	0.07	0.07	0.09	0.12	0.16	0.21	0.25	0.24	0.33	0.28	0.29	0.30	0.34	0.17	0.15
H_2O	1.32	1.47	1.22	1.10	0.91	0.56	0.33	0.24	0.33	0.57	0.29	0.28	0.24	1.00	1.03
-O=F	-0.03	-0.03	-0.04	-0.05	-0.07	-0.09	-0.11	-0.10	-0.14	-0.12	-0.12	-0.13	-0.14	-0.07	-0.06
Sum	100.84	100.15	101.05	100.05	99.73	98.90	98.50	98.44	97.88	97.80	97.82	99.73	99.64	100.83	100.22
P^{5+} *apfu*	0.000	0.000	0.003	0.004	0.008	0.043	0.018	0.023	0.000	0.000	0.074	0.003	0.000	0.036	0.040
Si^{4+}	2.910	2.814	2.785	2.734	2.668	2.641	2.711	2.656	2.385	2.275	2.123	2.008	1.948	2.458	2.513
As^{3+}	0.001	0.022	0.057	0.084	0.119	0.134	0.157	0.205	0.439	0.502	0.734	0.881	0.918	0.417	0.342
Sb^{3+}	0.000	0.000	0.014	0.022	0.046	0.046	0.046	0.061	0.072	0.069	0.038	0.053	0.059	0.033	0.033
Bi^{3+}	0.000	0.002	0.001	0.000	0.000	0.001	0.002	0.000	0.002	0.000	0.000	0.000	0.000	0.000	0.000
$^{[4]}Al^{3+}$	0.089	0.162	0.140	0.156	0.159	0.135	0.066	0.054	0.102	0.154	0.031	0.055	0.075	0.056	0.071
Σ*T*	3	3	3	3	3	3	3	3	3	3	3	3	3	3	3
B^{3+}	1	1	1	1	1	1	1	1	1	1	1	1	1	1	1
Al^{3+}	6.745	6.707	6.578	6.510	6.369	6.233	6.174	6.193	6.177	6.277	6.265	6.172	6.157	6.604	6.613
Ta^{5+}	0.000	0.000	0.051	0.082	0.154	0.273	0.330	0.323	0.291	0.115	0.192	0.159	0.181	0.001	0.005
Nb^{5+}	0.000	0.000	0.035	0.053	0.062	0.047	0.054	0.059	0.036	0.127	0.009	0.091	0.070	0.000	0.006
Ti^{4+}	0.000	0.000	0.000	0.001	0.002	0.003	0.000	0.000	0.000	0.000	0.001	0.001	0.011	0.000	0.000
Fe^{2+}	0.002	0.023	0.041	0.038	0.063	0.064	0.042	0.011	0.031	0.021	0.039	0.029	0.024	0.030	0.027
Mn^{2+}	0.000	0.000	0.001	0.002	0.003	0.004	0.001	0.002	0.005	0.006	0.001	0.000	0.000	0.002	0.002
Mg^{2+}	0.001	0.013	0.004	0.001	0.003	0.000	0.000	0.000	0.000	0.000	0.000	0.000	0.000	0.000	0.000
K^+	0.001	0.002	0.000	0.001	0.000	0.000	0.003	0.001	0.000	0.000	0.000	0.003	0.000	0.000	0.001
Σ*M*	6.750	6.745	6.711	6.690	6.655	6.625	6.603	6.588	6.541	6.547	6.507	6.454	6.443	6.637	6.653
O^{2-}	17.155	17.031	17.122	17.144	17.179	17.359	17.481	17.482	17.137	16.944	16.926	16.776	16.742	16.863	16.920
OH^-	0.824	0.924	0.779	0.713	0.605	0.391	0.230	0.172	0.238	0.394	0.205	0.191	0.168	0.636	0.659
F^-	0.021	0.021	0.027	0.037	0.051	0.069	0.084	0.080	0.111	0.092	0.096	0.098	0.112	0.051	0.046
Σ anions	17.999	17.976	17.928	17.894	17.836	17.819	17.795	17.734	17.487	17.429	17.228	17.066	17.023	17.550	17.625

vidually and interpret the relationships between mineral compositions and textures.

The magmatic assemblage

The textural pattern and order of crystallization (Fig. 10) show an early, primary, presumably magmatic assemblage formed by the crystallization from the contact inward of the succesive border, wall, intermediate and core or central paragenesis in the most fractionated dikes. These mineral associations are in approximately the order of formation: dravite + fluorapatite, schorl + quartz + plagioclase + elbaite (pollucite, gahnite) + rossmanite, quartz + elbaite + plagioclase + muscovite ± beryl ± columbite, quartz ± elbaite. The enrichment is particularly noteworthy in the zoning of tourmaline, which follows evolutionary trends reported at other localities for evolved rare-element pegmatites, accentuated by the high contents of Mn (Jolliff *et al.* 1986, Selway *et al.* 1999). Preservation of the inclusions of pollucite and gahnite strongly suggests that the inner parts of the tourmaline crystals have retained their

pristine magmatic composition. The accessory presence of beryl, columbite–(Mn) showing zoning to tantalite–(Mn) at very high values of Mn/(Mn+Fe), and the high whole–rock As and Sb contents, are all lines of evidence favoring the highly evolved composition of the melt.

The metamorphic overprint

The magmatic assemblage was affected by medium–pressure metamorphism, resulting in the occurrence of Ca–enriched plagioclase and fluorapatite, formation of Fe–enriched tourmaline + quartz + dumortierite assemblages, the partial reworking of columbite and the breakdown of a (Sb-As)–rich phase, both providing Nb-Ta-As-Sb for the crystallization of holtite, the formation of kyanite (most probably at the expense of

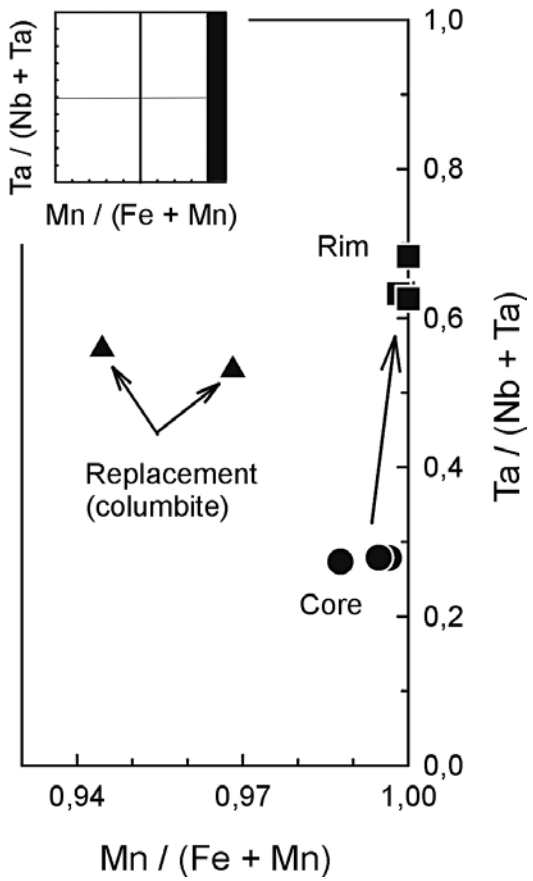

FIG. 9. Diagram showing the compositional variation of the columbite-group minerals from Virorco pegmatitic dikes in the columbite quadrilateral.

TABLE 5. REPRESENTATIVE COMPOSITIONS OF COLUMBITE–TANTALITE IN SAMPLE Vi06

	core		rim		replacement	
WO_3 wt.%	0.01	0.02	0.05	0.05	0.00	0.03
Ta_2O_5	31.39	31.02	60.60	64.44	53.42	53.24
Nb_2O_5	48.90	49.61	21.78	17.98	25.41	28.31
UO_2	0.15	0.12	0.00	0.12	0.26	0.01
SnO_2	0.10	0.07	0.11	0.25	0.01	0.04
ZrO_2	0.10	0.05	0.14	0.41	0.05	0.06
TiO_2	0.07	0.16	0.01	0.06	0.03	0.02
Y_2O_3	0.08	0.08	0.09	0.03	0.05	0.09
FeO	0.10	0.25	0.00	0.01	0.92	0.55
MnO	18.69	19.01	16.27	15.70	15.63	16.38
Total	99.59	100.39	99.05	99.05	95.78	98.73
F*	0.43	0.38	0.63	0.60	0.49	0.55
W *apfu*	0.000	0.000	0.001	0.001	0.000	0.001
Ta	0.548	0.534	1.227	1.336	1.085	1.041
Nb	1.418	1.419	0.733	0.620	0.858	0.920
U	0.002	0.002	0.000	0.002	0.004	0.000
Sn	0.003	0.002	0.003	0.007	0.000	0.001
Zr	0.003	0.002	0.005	0.015	0.002	0.002
Ti	0.003	0.007	0.001	0.003	0.002	0.001
Y	0.003	0.003	0.003	0.001	0.002	0.003
Fe^{2+}	0.005	0.013	0.000	0.001	0.058	0.033
Mn	1.015	1.019	1.026	1.014	0.989	0.997
O	5.961	5.943	5.953	5.964	5.924	5.949

* artificially induced values due to overlap with Ta. The composition is recalculated on the basis of three cations per formula unit.

TABLE 6. REPRESENTATIVE COMPOSITIONS OF BERYL

Sample	VI02-9	VI104-8	Vi03	Vi03
Point	9	17	28	29
SiO_2 wt.%	67.46	66.85	68.54	68.23
Cr_2O_3	0.10	0.04	0.02	0
Al_2O_3	18.00	18.45	18.46	18.55
ZnO	0.10	0.00	0.01	0
NiO	0.00	0.10	0.02	0
FeO	0.20	0.00	0.08	0.08
MgO	0.10	0.00	0.02	0
BeO*	13.94	13.90	14.17	14.12
Cs_2O	n.a.	n.a.	0.47	0.48
Rb_2O	n.a.	n.a.	0.09	0.07
Na_2O	0.10	0.29	0.18	0.12
Total	100.00	99.83	102.06	101.65
Si *apfu*	6.047	6.004	6.042	6.035
Cr	0.007	0.003	0.001	0.000
Al	1.901	1.953	1.918	1.934
Zn	0.007	0.000	0.001	0.000
Ni	0.000	0.007	0.001	0.000
Fe^{2+}	0.015	0.000	0.006	0.006
Mg	0.013	0.000	0.003	0.000
Be	3	3	3	3
Cs	-	-	0.018	0.018
Rb	-	-	0.005	0.004
Na	0.017	0.051	0.031	0.021
SUM	11.007	11.032	11.026	11.018

The amounts of S, P, Ti, V, Mn, Ba, Ni, K, Cl and F are below the detection limit; n.a.: not analyzed. * Calculated from stoichiometry.
The formula is calculated on the basis of 18 anions.

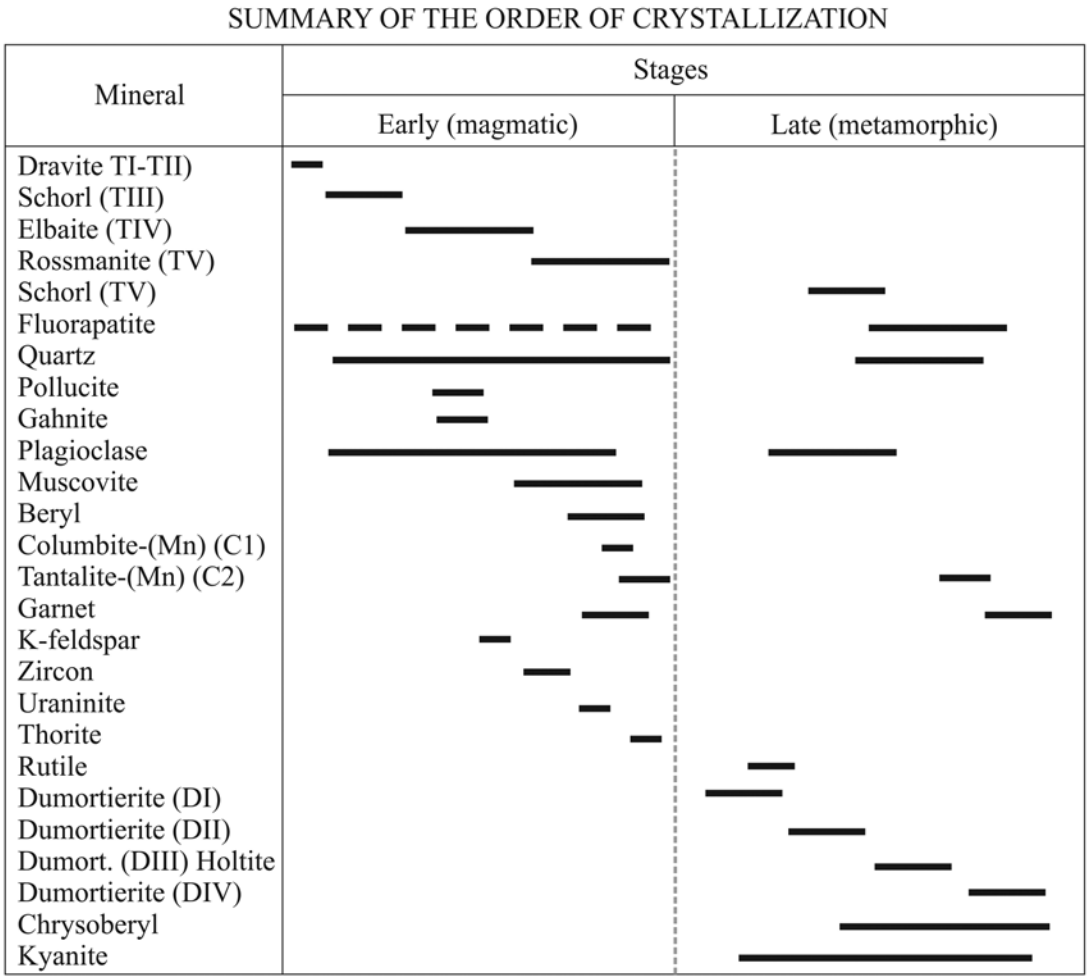

FIG. 10. Sequence of crystallization of minerals in the Virorco pegmatite dikes.

albite + muscovite or tourmaline), and also the breakdown of beryl and the crystallization of chrysoberyl + quartz. The latest minerals to crystallize were dumortierite (all four generations), fluorapatite and garnet. It is very likely that the crystallization of the metamorphic association was favored by the presence of a fluid phase, eventually with some remobilized boron component, and with Fe contamination from the host rock, which produced a Fe–rich tourmaline rim (Tur V) at the latest stage. It is not clear whether holmquistite in the dike exocontact is a result of fluid exchange between host rock and dikes soon after intrusion, or during the metamorphic overprint. The pressure conditions of metamorphism in the kyanite field generally agree with the maximum of 6.8 kbar obtained by Delpino *et al*. (2007) for the mylonitic event that deformed the metamorphic rocks of the area.

The source of the melt

The chemical composition of the dikes shows that the melt was strongly peraluminous, highly boron–enriched, and possibly F–enriched, very depleted in Na, K, and with a strong negative Eu anomaly, but remarkably enriched in Rb and Cs compared to average upper crust. The melt also contained high contents of Nb, Ta, Be, Cs, Sb and As with respect to normal contents of common peraluminous granites of "low and intermediate phosphorus", as quoted by Linnen & Cuney (2004). It is unlikely that the melt with the observed chemical composition could originate by partial melting of pelitic protholiths, was interpreted in some other occurrences of abyssal and BBe–enriched pegmatites (Grew *et al*. 2006, Cempírek & Novák 2006, Wadoski *et al*. 2011) or boron–bearing melts derived

from the partial melting of granulites (*e.g.*, Cempírek *et al.* 2010). However, a residual melt extracted from a rare–element parental pegmatite, similar to the one that outcrops 2.5 km to the north, would be able to produce a similar composition after most of its crystallization was complete. The possibility of formation of the dikes by infiltration–driven alteration caused by a polyphase boron–rich aqueous fluid, as was interpreted in the dikes hosted in kyanite quartzite and kyanite-mica schists from the Singhbhum Shear Zone, India (Sengupta *et al.* 2011), is unlikely in Virorco, *e.g.*, because of different geological settings (basic host–rock crosscut by younger dikes at Virorco), the pegmatite–like chemical and mineralogical signature of the Virorco dikes, the pegmatite zoning, and the compositional trend in magmatic minerals.

There was little retrogression following metamorphism, as is common in this kind of pegmatites (Cempírek & Novák 2006). The succession of assemblages in the Virorco dikes is in general agreement with the proposed geological evolution for the Pampean pegmatite province (Galliski 2009). This sequence involves the development of a belt of rare–element pegmatites in a continental collision tectonic setting, followed by stacking of basement slabs toward the suture zone and the rapid denudation of the entire pile. A tectonically active setting for the San Luis Range after the supposed emplacement of the dumortierite–bearing pegmatites is documented by the Ar–Ar age of muscovite from a sheared kyanite - staurolite - muscovite ± sillimanite pegmatite located 24 km to the north of Virorco dated at 375±1 Ma (Sims *et al.* 1998).

TABLE 7. SELECTED COMPOSITIONS OF MUSCOVITE

	VI104-1	VI104-4	VI03-5	VI104-7	VI114-5
SiO_2 wt.%	44.94	43.87	43.83	45.02	45.21
TiO_2	0.00	0.00	0.01	0.02	0.00
Al_2O_3	36.14	37.63	38.06	38.83	35.60
Fe_2O_3	0.00	0.00	0.00	0.00	0.00
FeO	0.35	0.22	0.19	0.29	0.91
MnO	0.11	0.03	0.03	0.01	0.01
MgO	0.00	0.01	0.01	0.01	0.18
CaO	0.02	0.00	0.00	0.00	0.02
Na_2O	1.43	1.11	1.16	1.59	1.45
K_2O	9.27	8.41	8.32	6.94	9.00
F	0.10	0.31	0.29	0.04	0.00
Cl	0.01	0.02	0.00	0.00	0.00
H_2O	4.35	4.23	4.27	4.48	4.40
O = F, Cl	0.04	0.14	0.12	0.02	0.00
Total	96.72	95.84	96.17	97.23	96.78
Si *apfu*	6.122	5.997	5.967	6.004	6.156
Al	1.878	2.003	2.033	1.996	1.844
Sum *T*	8.000	8.000	8.000	8.000	8.000
Al	3.920	4.055	4.069	4.102	3.864
Ti	0.000	0.000	0.001	0.002	0.000
Fe^{3+}	0.000	0.000	0.000	0.000	0.000
Fe^{2+}	0.040	0.025	0.022	0.032	0.104
Mn	0.013	0.003	0.003	0.001	0.001
Mg	0.000	0.002	0.002	0.002	0.037
Ca	0.003	0.000	0.000	0.000	0.003
Na	0.378	0.294	0.306	0.411	0.383
K	1.611	1.467	1.445	1.181	1.563
CAT SUM	13.965	13.846	13.848	13.731	13.955
F	0.086	0.268	0.250	0.034	0.000
Cl	0.005	0.009	0.000	0.000	0.000
OH	3.955	3.861	3.875	3.983	4.000

The number of ions is based on 24 (O, OH, F, Cl).

TABLE 8. SELECTED COMPOSITIONS OF GARNET

	VI104 -10	VI109 -42	VI109 -43	VI109 -45	VI114 -77	VI114 -79
SiO_2 wt.%	37.25	34.19	34.50	34.65	34.76	35.32
TiO_2	0.00	0.00	0.00	0.00	0.00	0.00
Al_2O_3	20.66	20.94	20.79	20.62	20.66	20.79
Cr_2O_3	0.05	0.00	0.00	0.03	0.00	0.00
FeO	2.61	3.74	2.87	4.15	1.69	4.06
MnO	39.51	37.93	38.15	36.76	39.43	36.98
MgO	0.00	0.00	0.01	0.02	0.00	0.01
CaO	0.78	0.48	0.55	0.62	0.44	0.73
Na_2O	0.09	0.03	0.01	0.01	0.00	0.03
FeO_{calc}	2.61	1.80	1.93	3.41	1.15	3.78
$Fe_2O_{3\ calc}$	0.00	2.16	1.04	0.82	0.60	0.32
Total	100.90	97.53	96.98	96.91	97.04	97.95
Si *apfu*	3.032	2.889	2.926	2.940	2.947	2.963
^{IV}Al	0.000	0.111	0.074	0.060	0.053	0.037
^{VI}Al	1.981	1.973	2.003	2.001	2.009	2.016
Fe^{3+}	0.000	0.137	0.066	0.052	0.038	0.020
Ti	0.000	0.000	0.000	0.000	0.000	0.000
Cr	0.003	0.000	0.000	0.002	0.000	0.000
Fe^{2+}	0.178	0.127	0.137	0.242	0.082	0.265
Mg	0.000	0.000	0.001	0.003	0.000	0.001
Mn	2.724	2.715	2.741	2.642	2.831	2.627
Ca	0.068	0.043	0.050	0.056	0.040	0.066
Na	0.014	0.005	0.002	0.002	0.000	0.005
X Alm	5.98	4.41	8.24	9.98	5.81	8.95
X Adr	0.00	1.51	1.64	1.78	1.31	1.01
X Grs	2.13	0.00	0.00	0.00	0.00	1.21
X Prp	0.00	0.00	0.04	0.08	0.00	0.04
X Sps	91.73	94.08	90.08	88.05	92.88	88.79
X Uv	0.16	0.00	0.00	0.10	0.00	0.00

Dumortierite – holtite relationship

Dumortierite and holtite are isostructural members of the dumortierite group and form extensive solid–solutions (Groat *et al.* 2009); their occurrences are closely associated. Holtite, originally described from Greenbushes, Australia (Pryce 1971, Hoskins *et al.* 1989) as approximately (Al,Ta, □) $Al_6(BO_3)(Si,Sb^{3+},As^{3+})_{\Sigma 3}O12(O,OH,\square)_{\Sigma 3}$, has rather poorly defined end–member composition. Groat *et al.* (2009) found two independent substitutions $^{M1}Ta_3\square 2^{M1}Al_5$ and $\square(As,Sb)_3(AlSi_3)_{-1}$, leading to the end–member compositions $(Ta_{0.6}\square_{0.4})Al_6BSi_3O_{18}$ and $Al_6B(As,Sb)_3O_{15}$, respectively. Assuming these compositions, dumorti-

erite with (Ta,Nb) > 0.3 *apfu* or (As,Sb) > 1.5 *apfu* can be classified as holtite. Pieczka *et al*. (2011) describing the minerals that occurs at Szklary pegmatite, considered as holtite compositions with Ta + Nb + Ti > 0.25 *apfu* and dumortierite as compositions with Ta + Nb + Ti <0.1 *apfu*.

In Virorco, the Ta–rich dumortierite III, with Ta + Nb contents of ~0.4 *apfu*, satisfies both criteria and can be classified as holtite. On the other hand, the As–rich dumortierite IV, with a very high content of As (up to 1 *apfu*), must still be regarded as an As–rich variety of dumortierite. Similar contents of As were recently documented in few grains of otherwise Sb–rich holtite from Szklary, Poland (Pieczka *et al*. 2011).

Comparison with other occurrences of holtite

Holtite is a fairly rare mineral, only found in three localities other than Virorco: Greenbushes, Australia (Pryce 1971), Vasin-Myl'k, Voron'i Tundry, Kola Peninsula, Russia (Voloshin *et al*. 1977) and Szklary, Poland (Pieczka *et al*. 2011). Its origin is non–uniform and rather unclear.

In the Greenbushes occurrence, holtite, in association with stibiotantalite, tantalite and minor tourmaline, microlite and quartz, is known from small (2-15 mm) pebbles in alluvium of the Greenbushes pegmatite. It is present mainly as intergrown prisms and acicular coatings on stibiotantalite and as parallel acicular to asbestiform replacements of tantalite; some pure holtite occurs as hard resinous pebbles composed of parallel needles, generally with S-shaped contortions attributed to shearing during fluid-driven replacement of tantalite (Pryce 1971). High-grade tantalum mineralization is restricted to the albite zone, especially concentrated in the tourmaline-rich parts, but tantalite it is also present in the quartz–spodumene–apatite zone, which forms the topmost part and wall zones of the pegmatite. The pegmatite crystallized synchronously with an episode of upper amphibolite facies metamorphism and shows widespread signs of deformation (Partington 1990, Partington *et al*. 1995).

The holtite from Vasin–Myl'k Mountain comes from a flat-dipping zoned pegmatite cross-cutting amphibolite. Holtite was found in the dike center, in a zone containing coarse-grained and blocky quartz, microcline, albite of cleavelandite habit, spodumene, amblygonite, pollucite and fine-grained lepidolite, especially in nests and veins containing quartz, albite, elbaite, amblygonite and lepidolite on fractures of blocky microcline or pollucite. It forms coarse-grained prismatic crystals up to 5 cm long, commonly associated with zircon. Voloshin *et al*. (1987) distinguished a fibrous, Sb-rich variety of holtite, referred to as holtite II. It overgrows the prismatic crystals of holtite I, or it replaces stibiotantalite and microlite on grain borders and fractures. Holtite II is the youngest Ta-phase in the assemblage. Holtite I is locally replaced by stibiotantalite, microlite or kolfanite (in an assemblage with mitridatite), but it is never associated with primary oxides of Ta (tantalite, microlite, simpsonite) (Voloshin *et al*. 1977, 1982, 1987).

In the Szklary pegmatite, Pieczka *et al*. (2011) (see also Pieczka 2010) attributed the origin of holtite to the primary crystallization of a parental melt enriched in Ta, Nb, Sb, As, Al and B, and with low fugacity of sulfur. The pegmatite also contains cordierite in the border zone and chrysoberyl associated with muscovite or K-feldspar + quartz, suggesting that it could have been affected by metamorphism. The pegmatite minerals also include albite, tourmaline, spessartine, a number of Ta–Nb oxides, beusite and Mn-rich fluorapatite; the K-feldspar is rich in P_2O_5 (0.5–0.6 wt.%). Pieczka *et al*. (2011) proposed that the origin of all the parageneses could be magmatic.

There are several features common to all known occurrences of holtite. First, all the pegmatites crosscut mafic rocks and on two of them mass exchange with the host rock and metamorphic overprint were observed (Greenbushes, Virorco); however, none of these features could be the result of a uniform process crucial for holtite stabilization at all localities. However, the geochemically striking feature is the abundance of P, and in later stage also of Ca and Mn, in all the holtite-bearing pegmatites: abundant Mn-enriched fluorapatite in the quartz–spodumene zone in Greenbushes, amblygonite and secondary phosphates at Vasil Mil'k Mountain, beusite and Mn-rich fluorapatite in Szklary (holtite is rarely enclosed in Mn oxides, possibly after beusite ?), and late fluorapatite and spessartine enclosing holtite in Virorco. Phosphorus in known to be a strong complexing agent for Al, causing a decrease in polymerization and viscosity of peraluminous melts (*e.g.*, Pichavant *et al*. 1992, Mysen *et al*. 1999). Competition of phosphorus with (Ta, Nb) for Al in coupled substitutions in zircon was experimentally observed (van Lichtervelde *et al*. 2011). We suggest that the high phosphorus content, significantly increasing peraluminosity of the residual pegmatite-forming melt, is the key factor that makes Al available for stabilization of dumortierite-group phases. As P cannot enter their structure, this mechanism also allows the incorporation of the available structurally convenient cations (Ta, As, Nb).

At Greenbushes, Vasil–Mil'k, and Szklary, early holtite forms rather thick prismatic crystals of undeformed crystals which seem to be primary; however, deformed lensoidal aggregates of secondary fibrous (asbestiform) holtite were also observed at all localities (in Virorco they prevail), suggesting postmagmatic metamorphic remobilization of Al, Ta and As. Deformation, especially at Greenbushes and Virorco (and on a small scale, possibly at Vasil–Mil'k and Szklary) could be a possible trigger responsible for destabilization of primary phases (*e.g.*, phosphates, Ta oxides) and local generation of Al- and P-rich melt or fluid. The dumortierite and holtite of the Virorco pegmatites are consid-

ered of metamophic origin on the basis of the textural and microstructural patterns described. The evolution of the chemical compositions from dumortierite I to IV (Fig. 7) with increasing contents of Ta + Nb from dumortierite II to holtite, which evolves to (Ta–Nb)-poor (As + Sb + Bi)-rich dumortierite, follows approximately the same trend as in the Szklary pegmatite. Such an evolution could be explained, from a metamophic point of view, as a result of successive dissolution of zoned columbite-group minerals, followed by the breakdown of some Sb- and As-rich phase(s) (*e.g.,* stibarsen or löllingite), or of the preferred partitioning of Ta over Nb in holtite and its earlier exhaustion from the melt.

Conclusions

The dumortierite-bearing dikes of Virorco were formed in a two-stage process. The magmatic stage originated a zoned assemblage of pegmatite-forming minerals crystallized possibly from a highly fractionated, fluxed residual melt, enriched in B, Li, Be, Ta and Cs which probably was extracted from a rare-element parental pegmatite, after most of its crystallization was complete. The metamorphic stage overlapped the previous one with a prograde medium- to high-pressure assemblage developing kyanite, chrysoberyl, dumortierite and holtite as the most significant minerals.

Acknowledgements

The authors are very grateful to C.A. Heinrich for the use of the electron microprobe and LA– ICP–MS facilities of the ETH Zurich, and to P. Černý of the University of Manitoba for the use of the electron microprobe. Grants PIP 5907 and 857 of CONICET and PICT 21638 of FONCYT financed the research, as well as the grant GACR P210/10/0743. At an early stage, we benefitted from the kind help of Ed Grew in the recognition of holtite. D. London provided alternative insights for interpreting genetic constraints of this occurrence and relevant references. The authors are very grateful for the constructive reviews of Donald Burt and particularly of Ed Grew, for the generous assistance in improving the clarity and the writing of the manuscript. The editorial comments of Robert F. Martin and the editorial handling of David London are much appreciated.

The authors are especially happy to dedicate this paper to Petr Černý in recognition of his lifelong noteworthy contributions to the world of granitic pegmatites and the inspiration he has provided us.

References

Alfonso, P., Melgarejo, J.C., Yusta I. & Velasco, F. (2003): Geochemistry of feldspars and muscovite in granitic pegmatite from the Cap de Creus field, Catalonia, Spain. *Can. Mineral.* **41**, 103-116.

Cempírek, J. & Novák, M. (2006): Mineralogy of dumortierite-bearing abyssal pegmatites at Starkoč and Běstvina, Kutná Hora crystalline complex. *J. Czech Geol. Soc.* **51**(3-4), 259-270.

Cempírek, J., Novák, M., Dolníček, Kotková, J. & Škoda, R. (2010): Crystal chemistry and origin of grandidierite, ominelite, boralsilite, and werdingite from the Bory Granulite Massif, Czech Republic. *Am. Mineral.* **95**, 1533-1547.

Černý, P. & Ercit, T.S. (2005): The classification of granitic pegmatites revisited. *Can. Mineral.* **43**, 2005-2026.

Černý, P., Novák, M. & Chapman, R. (1992): Effect of sillimanite-grade metamorphism and shearing on Nb–Ta oxide minerals in granitic pegmatites: Maršíkov, northern Moravia, Czechoslovakia. *Can. Mineral.* **30**, 699-718.

Černý, P., Teertstra, D.K., Chapman, R., Fryer, B.J., Longstaffe, F.J., Wang, X.-J., Chackowsky, L.E. & Meintzer, R.E. (1994): Mineralogy of extreme fractionation in rare-element pegmatites at Red Cross Lake, Manitoba, Canada. Int. Mineral. Assoc., 16th Gen. Meeting (Pisa), Abstr., 67.

Deer, W.A., Howie, R.A. & Zussman, J. (1997): *Rock-Forming Minerals*. 1. *Ortho- and Ring Silicates*. John Wiley & Sons Inc., New York, N.Y.

Delpino, S.H., Bjerg, E., Ferracutti, G.R. & Mogessie, A. (2007): Counterclockwise tectonometamorphic evolution of the Pringles metamorphic complex, Sierras Pampeanas of San Luis (Argentina). *J. S. Am. Earth Sci.* **23**, 147-175.

Franz, G. & Morteani, G. (2002): Be-minerals: synthesis, stability, and occurrence in metamorphic rocks. *In* Beryllium: Mineralogy, Petrology and Geochemistry (E.S. Grew, ed.). *Rev. Mineral.* **50**, 551-589.

Galliski, M.A. (2009): The Pampean pegmatite province, Argentina: a review. *In* Contributions of the 4th International Symposium on Granitic Pegmatites. *Estudos Geológicos* **19**(2), 30-34.

Gay, H.D. & Galliski, M.A. (1978): Dumortierita, crisoberilo y minerales asociados de Virorco, San Luis. *VII Cong. Geol. Argentino* **II**, 327-335.

González Bonorino, F. (1961): Petrología de algunos cuerpos básicos de San Luis y las granulitas asociadas. *Rev. Asoc. Geol. Argentina* **19**(3), 135-150.

Grew, E.S. (1981): Surinamite, taaffeite and beryllian sapphirine from pegmatites in granulite-facies rocks of Casey Bay, Enderby Land, Antarctica. *Am. Mineral.* **66**, 1022-1033.

Grew, E.S., Yates, M.G., Shearer, C.K., Haggerty, J.J., Sheraton, J.W. & Sandiford, M. (2006): Beryllium and other trace elements in paragneisses and anatectic dikes of the ultrahigh –temperature Napier Complex, Enderby Land, East Antarctica: the role of sapphirine. *J. Petrol.* **47**, 859-882.

GROAT, L.A., GREW, E.S., EVANS, R.J., PIECZKA, A. & ERCIT, T.S. (2009): The crystal chemistry of holtite. *Mineral. Mag.* **73**, 1033-1050.

HENRY, D.J., DUTROW, B.L. & SELVERSTONE, J. (2002): Compositional asymmetry in replacement tourmaline – an example from the Tauern Window, Eastern Alps. *Geol. Mater. Res.* **4**(2), 1-18.

HENRY, D.J., NOVÁK, M., HAWTHORNE, F.C., ERTL, A., DUTROW, B.L., UHER, P. & PEZZOTTA, F. (2011): Nomenclature of the tourmaline-supergroup minerals. *Am. Mineral.* **96**, 895-913.

HOSKINS, B.F., MUMME, W.G. & PRYCE, M.W. (1989): Holtite, $(Si_{2.25}Sb_{0.75})B$ $[(Al_6(Al_{0.43}Ta_{0.27}\square_{0.30})O_{15}(O,OH)_{2.25}]$: crystal structure and crystal chemistry. *Mineral. Mag.* **53**, 457-463.

JOLLIFF, B.L., PAPIKE, J.J. & SHEARER, C.K. (1986): Tourmaline as a recorder of pegmatite evolution: Bob Ingersoll pegmatite, Black Hills, South Dakota. *Am. Mineral.* **71**, 472-500.

KALT, A., SCHREYER, W., LUDWIG, T., PROWATKE, S., BERNHARDT, H.-J. & ERTL, A. (2001): Complete solid solution between magnesian schorl and lithian excess-boron olenite in a pegmatite from Koralpe (eastern Alps, Austria). *Eur. J. Mineral.* **13**, 1191-1205.

LINNEN, R.L. & CUNEY, M. (2004): Granite-related rare-element deposits and experimental constraints on Ta–Nb–W–Sn–Zr–Hf mineralization. *In* Rare-Element Geochemistry and Mineral Deposits, (R.L. Linnen & I.M. Samson, eds.). *Geol. Assoc. Can., Short Courses Notes* **17**, 45-68.

LOSERT, J. (1956): Dumortierite from the pegmatites and migmatites in the region of Kutná Hora. Rozpravy Československ. Akad. Věd. **66**, 1-48 (In Czech, with summary in English).

MARSCHALL, H.R., ALTHERR, R., KALT, A. & LUDWIG, T. (2008): Detrital, metamorphic and metasomatic tourmaline in high-pressure metasediments from Syros (Greece): intra-grain boron isotope patterns determined by secondary-ion mass spectrometry. *Contrib. Mineral. Petrol.* **155**, 703-717.

MCDONOUGH, W.F. & SUN, S.-S. (1995): The composition of the Earth. *Chem. Geol.* **120**, 223-253.

MORGAN, G.B. VI & LONDON, D. (1987): Alteration of amphibolitic wallrocks around the Tanco rare-element pegmatite, Bernic Lake, Manitoba. *Am. Mineral.* **72**, 1097-1121.

MYSEN, B.O., HOLTZ, F., PICHAVANT, M., BENY, J.-M. & MONTEL, J.-M. (1999): The effect of temperature and bulk composition on the solution mechanism of phosphorus in peraluminous haplogranitic magma. *Am. Mineral.* **84**, 1336-1345.

NĚMEC, D. (1989): Lithium aluminosilicates in pegmatites affected by stress. *Chem. Erde* **49**, 167-172.

PARTINGTON, G.A. (1990): Environmental and structural control on the intrusion of the giant rare-metal pegmatite at Greenbushes, Western Australia. *Econ. Geol.* **85**, 437-456.

PARTINGTON, G.A., MCNAUGHTON, N.J. & WILLIAMS, I.S. (1995): A review of the geology, mineralization and geochronology of the Greenbushes pegmatite, Western Australia. *Econ. Geol.* **90**, 616-635.

PASTORE, F. & RUIZ HUIDOBRO, O. (1952): Descripción Geológica de la Hoja 24g Saladillo, Provincia de San Luis. *Boletín de la Dirección Nacional de Minería* **78**,1-63.

PICHAVANT, M., MONTEL, J.-M. & RICHARD, L.R. (1992): Apatite solubility in peraluminous liquids: experimental data and an extension of the Harrison–Watson model. *Geochim. Cosmochim. Acta* **56**, 3855-3861.

PIECZKA, A. (2010): Primary Nb–Ta minerals in the Szklary pegmatite, Poland: new insights into controls of crystals chemistry and crystallization sequences. *Am. Mineral.* **95**, 1478-1492.

PIECZKA, A., GREW, E.S., GROAT, L.A. & EVANS, R.J. (2011): Holtite and dumortierite from Szklary pegmatite, Lower Silesia, Poland. *Mineral. Mag.* **75**, 303-315.

POUCHOU, J.L. & PICHOIR, F. (1985): "PAP" ($\phi\rho$ Z) correction procedure for improved quantitative microanalysis. *In* Microbeam Analysis (J. T. Armstrong, ed.). San Francisco Press, San Francisco, California (104-106).

PRYCE, M.W. (1971) Holtite: a new mineral allied to dumortierite. *Mineral. Mag.* **38**, 21-25.

SELWAY, J.B., NOVÁK, M., ČERNÝ, P. & HAWTHORNE, F.C. (1999): Compositional evolution of tourmaline in lepidolite-subtype pegmatites. *Eur. J. Mineral.* **11**, 569-584.

SELWAY, J.B. & XIONG JIANG (2002): Tourmaline-recalculation software quoted in Tindle *et al.* (2002). http://www.open.ac.uk/earth-research/tindle/.

SENGUPTA, N., SENGUPTA, P. & SACHAN, H. K. (2011): Aluminous and alkali-deficient tourmaline from the Singhbhum Shear Zone, East Indian shield: insight for polyphase boron infiltration during regional metamorphism. *Am. Mineral.* **96**, 752-767.

SIMS, J.P., IRELAND, T.R., CAMACHO, A., LYONS, P., PIETERS, R.G., STUART-SMITH, P.G. & MIRÓ, R. (1998): U–Pb, Th–Pb and Ar–Ar geochronology from the Southern Sierras Pampeanas, Argentina: implications for the Paleozoic tectonic evolution of the western Gondwana margin. *In* The Proto-Andean Margin of Gondwana (R.J. Pankhurst & C.A. Rapela, eds.). *Geol. Soc., Spec. Publ.* **142**, 259-281.

SIMS, J.P., SKIRROW, R.G., STUART-SMITH, P.G. & LYONS, P. (1997): Informe geológico y metalogénico de las Sierras de San Luis y Comechingones (Provincias de San Luis y Córdoba), 1:250000. Anales XXVIII, Instituto de Geología y Recursos Minerales, SEGEMAR, Buenos Aires, Argentina.

STILLING, A., ČERNÝ, P. & VANSTONE, P. (2006): The Tanco pegmatite at Bernic Lake, Manitoba. XVI. Zonal and bulk compositions and their petrogenetic significance. *Can. Mineral.* **44**, 599-623.

TAYLOR, S.R. & MCLENNAN, S.M. (1995): The geochemical evolution of the continental crust. *Rev. Geophys.* **33**, 241-265.

TRUEMAN, D.L. & ČERNÝ, P. (1982): Exploration for rare-element granitic pegmatites. *In* Granitic Pegmatites in Science and Industry (P. Černý, ed.). *Mineral. Assoc. Canada, Short Course Handbook* **8**, 463-494.

VAN HINSBERG, V.J., HENRY, D.J. & MARSCHAL, H.R. (2011): Tourmaline: and ideal indicator of its host environment. *Can. Mineral.* **49**, 1-16.

VAN LICHTERVELDE, M., HOLTZ, F., DZIONY, W., LUDWIG, T. & MEYER, H.-P. (2011): Incorporation mechanisms of Ta and Nb in zircon and implications for pegmatitic systems. *Am. Mineral.* **96**, 1079-1089.

VIEIRA, R., RODA-ROBLES, E., PESQUERA, A. & LIMA, A. (2011): Chemical variation and significance of micas from the Fregeneda–Almendra pegmatitic field (Central-Iberian Zone, Spain and Portugal). *Am. Mineral.* **96**, 637-645.

VOLOSHIN, A.V., GORDIENKO, V.V., GEL'MAN, E.M., ZORINA, M.L., ELINA, N.A., KUL'CHITSKAYA, E.A., MEN'SHIKOV, Y.P., POLEZHAEVA, L.I., RYZHOVA, R.I. , SOKOLOV, P.B. & UTOCHKINA, G.I. (1977): Holtite (first find in the USSR) and its interaction with other tantalum minerals in rare metal pegmatites. *Zap. Vses. Mineral. Obshchest.* **106**, 337-347 (in Russian).

VOLOSHIN, A.V., MEN'SHIKOV, YU.P., POLEZHAEVA, L.I. & LENTSI, A.A. (1982): Kolfanite, a new mineral from granite pegmatites of the Kola Peninsula. *Mineral. Zh.* 4, 90-95 (in Russian with English abstract).

VOLOSHIN, A.V., PAKHOMOVSKIY, YA.A. & ZALKIND, O.A. (1987): An investigation of the chemical composition and IR-spectroscopy of holtite. *In* Mineral'nyye Assotsiatsii i Mineraly Magmacheskikh Kompleksov Kol'skogo Polyostrova, Apatity, Kol'skiy Filial AN SSSR, 14-34 (in Russian).

WADOSKI, E.R., GREW, E.S. & YATES, M.G. (2011): Compositional evolution of tourmaline-supergroup minerals from granitic pegmatites in the Larsemann Hills, East Antarctica. *Can. Mineral.* **49**, 381-405.

ZEN, E-AN (1986): Aluminum enrichment in silicate melts by fractional crystallization: some mineralogic and petrographic constraints. *J. Petrol.* **27**, 1095-1117.

Received July 26, 2011, revised manuscript June 15, 2012.